NASA/TM—2017-219721

Methodologies for Root Locus and Loop Shaping Control Design With Comparisons

George Kopasakis
Glenn Research Center, Cleveland, Ohio

December 2017

NASA STI Program . . . in Profile

Since its founding, NASA has been dedicated to the advancement of aeronautics and space science. The NASA Scientific and Technical Information (STI) Program plays a key part in helping NASA maintain this important role.

The NASA STI Program operates under the auspices of the Agency Chief Information Officer. It collects, organizes, provides for archiving, and disseminates NASA's STI. The NASA STI Program provides access to the NASA Technical Report Server—Registered (NTRS Reg) and NASA Technical Report Server—Public (NTRS) thus providing one of the largest collections of aeronautical and space science STI in the world. Results are published in both non-NASA channels and by NASA in the NASA STI Report Series, which includes the following report types:

- TECHNICAL PUBLICATION. Reports of completed research or a major significant phase of research that present the results of NASA programs and include extensive data or theoretical analysis. Includes compilations of significant scientific and technical data and information deemed to be of continuing reference value. NASA counter-part of peer-reviewed formal professional papers, but has less stringent limitations on manuscript length and extent of graphic presentations.

- TECHNICAL MEMORANDUM. Scientific and technical findings that are preliminary or of specialized interest, e.g., "quick-release" reports, working papers, and bibliographies that contain minimal annotation. Does not contain extensive analysis.

- CONTRACTOR REPORT. Scientific and technical findings by NASA-sponsored contractors and grantees.

- CONFERENCE PUBLICATION. Collected papers from scientific and technical conferences, symposia, seminars, or other meetings sponsored or co-sponsored by NASA.

- SPECIAL PUBLICATION. Scientific, technical, or historical information from NASA programs, projects, and missions, often concerned with subjects having substantial public interest.

- TECHNICAL TRANSLATION. English-language translations of foreign scientific and technical material pertinent to NASA's mission.

For more information about the NASA STI program, see the following:

- Access the NASA STI program home page at http://www.sti.nasa.gov

- E-mail your question to help@sti.nasa.gov

- Fax your question to the NASA STI Information Desk at 757-864-6500

- Telephone the NASA STI Information Desk at 757-864-9658

- Write to:
  NASA STI Program
  Mail Stop 148
  NASA Langley Research Center
  Hampton, VA 23681-2199

NASA/TM—2017-219721

Methodologies for Root Locus and Loop Shaping Control Design With Comparisons

George Kopasakis
Glenn Research Center, Cleveland, Ohio

National Aeronautics and
Space Administration

Glenn Research Center
Cleveland, Ohio 44135

December 2017

Acknowledgments

The author would like to acknowledge Jonathan Litt of NASA GRC for his thorough review of the paper and many helpful comments.

This work was sponsored by the Airspace Operations and Safety Program at the NASA Glenn Research Center.

Level of Review: This material has been technically reviewed by technical management.

Available from

NASA STI Program
Mail Stop 148
NASA Langley Research Center
Hampton, VA 23681-2199

National Technical Information Service
5285 Port Royal Road
Springfield, VA 22161
703-605-6000

This report is available in electronic form at http://www.sti.nasa.gov/ and http://ntrs.nasa.gov/

Methodologies for Root Locus and Loop Shaping Control Design With Comparisons

George Kopasakis
National Aeronautics and Space Administration
Glenn Research Center
Cleveland, Ohio 44135

Abstract

This paper describes some basics for the root locus controls design method as well as for loop shaping, and establishes approaches to expedite the application of these two design methodologies to easily obtain control designs that meet requirements with superior performance. The two design approaches are compared for their ability to meet control design specifications and for ease of application using control design examples. These approaches are also compared with traditional Proportional Integral Derivative (PID) control in order to demonstrate the limitations of PID control. Robustness of these designs is be covered as it pertains to these control methodologies and for the example problems.

1.0 Introduction

Root locus (RL) controls design is about designing the open loop (OL) transfer function (TF) in order to locate the closed loop (CL) poles of the feedback system at the desired location on the s-plane, such that the control system design satisfies the performance objectives. In Loop Shaping controls design, the objective is also to shape the OL TF in the frequency domain to satisfy control system performance objectives/specs. In either case, the control law or the controller TF ends up being designed in this process.

Root Locus controls design is well covered in literature, as any book (Ref. 1) on classical controls theory will have a chapter or section devoted to this control design methodology. Where it gets a little complicated is how to best utilize the theory to come up with control designs that are relatively easy to implement, and also meet specifications with good performance, including high disturbance rejection and good stability margins. The RL controls theory is somewhat rigorous, which makes it difficult to apply. The approach that is covered here tries to maintain simplicity and practicality, so that the design process may become easier and more widely usable.

Loop Shaping (LS) controls design, which primarily involves the shaping of the OL transfer function (TF) in a feedback control system, is covered somewhat sparingly in text books or the approaches covered are sort of ad hoc and hard to generalize. References 2 and 3, present a LS controls design approach that is methodical. As covered in Reference 2, this control design technique achieves about as good performance as possible (i.e., response time specs, disturbance rejection, and stability margins) given the speed or rate limitation of the process or its actuation. The LS approach that is covered here is the same as that covered in these references, except that more practical considerations are provided here in order to further expedite and simplify the implementation process of the design.

Example designs using these RL and LS approaches covered here are also contrasted against traditional Proportional Integral Derivative (PID) control, in order to demonstrate the benefits of the approaches over PID control.

The paper is organized as follows. First, RL is applied to some simple control problems in order to identify certain patterns in the design process from which a simplified controls design approach can

emerge that can then be applied for more complicated control design problems. This is followed by the details of the LS control design technique, which is applied to the same control design example. Then the PID control design is discussed and compared to the RL and LS methods. Finally, some concluding remarks are offered.

2.0 An Approach for Root Locus Control Design

In RL controls system design the exact root locus trajectory can be computed by selecting the poles and zeros of the OL TF. The poles and zeros of the OL TF can be selected using calculations such as the angle and center of asymptotes, breakaway and break-in points, departure and arrival angles, etc. The OL proportional gain can be selected to place the CL poles at a desired location in the s-plane in order to satisfy control system performance objectives/specs. While the theory of RL controls design is structured and it can be used to achieve as good of a performance as any classical controls design method, its complexity makes it hard to apply for other than just simplified control problems. The attempt here is to dispense with much of the mathematical complexity and instead utilize practical or rule of thumb considerations, but still achieve about as good of a controls design as possible.

If the reader is unfamiliar with the basic concepts of RL, it is recommended to gain some basic insight by reading any linear systems or control systems book on the subject, which will make it easier to follow the concepts discussed in this paper; the assumption here is that the reader already has some basic familiarity with the subject area.

2.1 Root Locus Design Methodology Considerations

If the proportional gain, K, of the control system were to be increased starting from zero, the location of the CL poles would move, starting from their OL location, and as the proportional gain approaches infinity, the location of the CL poles approaches that of the OL zeros. The reason for this is because the CL TF (assuming unity feedback) is $T(s)=G(s)/[1+G(s)]=[KN(s)/D(s)]/[1+KN(s)/D(s)]$, where $G(s)$ is the OL TF and N(s), D(s) are the numerator and denominator polynomial expressions of G(s), respectively. By simplifying, $T(s)=KN(s)/[D(s)+KN(s)]$. From this expression, it can be seen (by inspection) that for a value of K near zero, the poles of the CL TF are the same as the OL poles, and for $K=\infty$, the poles of the CL TF are the same as the OL zeros, and for increasing gain values, these poles move towards the zeros.

Each of the poles in the system moves towards a distinct zero, with the extra poles moving to find zeros at infinity as the gain, K, approaches infinity (there are always extra zeros at infinity). The trajectory of the CL poles in the s-domain as the proportional gain is increased, is called the RL. The controller design for the RL involves either (a) finding the appropriate gain given a controller structure of poles and zeros, or (b) designing the appropriate control structure by choosing the pole and zero locations of the OL TF in order to shape the RL as desired, and then finding the appropriate gain for the desired CL pole locations that satisfies $1+KG(s) = 0$ and meets performance requirements. This is the well-known characteristic equation of the system. The design option that will be chosen here is (b), as in this case the maximum flexibility is offered to design a control system that meets the specs and achieves good performance.

Three basic RL rules are provided here that are essential to point out in order to facilitate the discussions. One, the RL is always symmetrical with respect to the real axis of the s-plane. Two, the portion of the RL on the real axis starts to the left of an odd number of poles and zeros. Three, the number of branches of the RL is equal to the number of poles and starts at the OL pole location (for $K=0$) and ends at the zeros (for $K=\infty$); the remaining poles go to infinity along asymptotes.

Say that the OL TF of the control system has only two poles, located anywhere on the real axis in the Left-Hand s-Plane (LHP), and for demonstration purposes lets pick their locations at s=-1,-2. Using MATLAB® (The MathWorks, Inc.), we can plot the RL as the gain K increases from 0 towards ∞, as shown in Figure 1. This can also be done by hand, by finding and plotting the roots of the polynomial $D(s)+KN(s)=0$ for different values of the gain K, as the gain increases from zero to infinity. In these figures the x's and o's indicate the location of the poles and zeros of the OL TF, respectively.

Notice in Figure 1 that the RL trajectory starts from the OL pole location, on the left of an odd number of poles and zeros (i.e., left of the rightmost pole), moves towards the middle and splits at s=-1.5, and moves away from the real axis towards ∞. Besides using MATLAB® or evaluating the CL TF and plotting it point-by-point, the root locus could have also been sketched by hand, by calculating center and angle of asymptotes, and break-away points. This will not be done here as the objective is to develop the skills to properly place poles and zeros to shape the RL using experience or intuition, more so than calculations. The commands used here are as follows: **s=tf('s'); G=1/((s+1)*(s+2)); rlocus(G)**. Notice the proportional gain K in the OL TF, G, is set to 1 for convenience as MATLAB® varies this gain from 0 to ∞, and as such a point selected on the RL (shown later) will display the actual OL gain, K, for that location. If we add another pole on the real axis in the LHP, the RL will look as shown in Figure 2. Notice that with three poles, the two rightmost will come together and split to cross the imaginary axis into the Right-Half Plane (RHP), while the third pole goes towards a zero at -∞. With the root locus crossing into the RHP it means that by increasing the gain, K, beyond some value, it will make the CL system response unstable. If a zero is added instead of a third pole, and if the zero is located in between the two-poles, then one pole will go to the zero (as K increases from 0 to ∞), while the other pole will move along the real axis towards the zero at -∞. Again, this can be easily ascertained without any calculations by knowing that the RL trajectory on the real axis starts to the left of an odd number of poles and zeros. On the other hand, if the zero is located to the left of both of the poles, the RL will look as shown in Figure 3. Notice the poles in this case meet at the RL region to the left of an odd number of poles and zeros. Because one pole needs to go to the zero at -∞, and because the RL needs to remain symmetrical with respect to the real axis, they come back together on the real axis, somewhere to the left of the leftmost zero (one zero in this case), and then they separate with one pole going to the zero location and the other to -∞. If one of the poles in the system depicted in Figure 3 was instead located on the real axis in the RHP, the RL will look the same, but shifted to the right, and in this case the system will be stable above a minimum value of the gain, K, since for small gain values in this case, the RL will be located in the RHP (unstable).

Exactly at what angle(s) the poles depart and at what location the poles come back together, etc., can be computed, but again the main objective here is to develop an intuition of how the root locus behaves by the addition of poles or zeros, rather than precisely determining these shapes. The general shape of the RL shown in Figure 3 will be crucial for more complicated control designs. By knowing how to bend and locate the RL trajectory to the left, it can be ensured that the system will remain stable for any value of gain, K, greater than zero. This is the case as long as the RL trajectory remains in the LHP. As will be seen later, by selecting the gain to locate the CL poles on the RL closer to the real axis in the LHP, the more damped the control system response will be. The distance from the origin to the RL determines how fast the system response will be (at least the initial response).

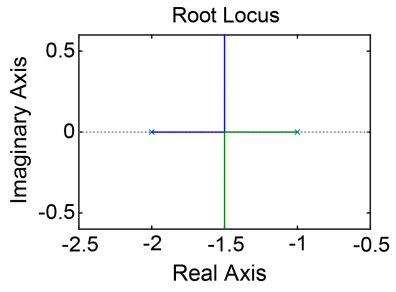

Figure 1.—Root locus of two pole system.

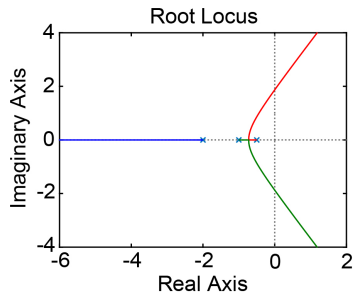

Figure 2.—Root locus of three pole system.

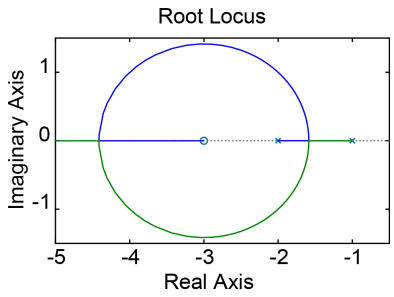

Figure 3.—Root locus of two poles and one zero to the left.

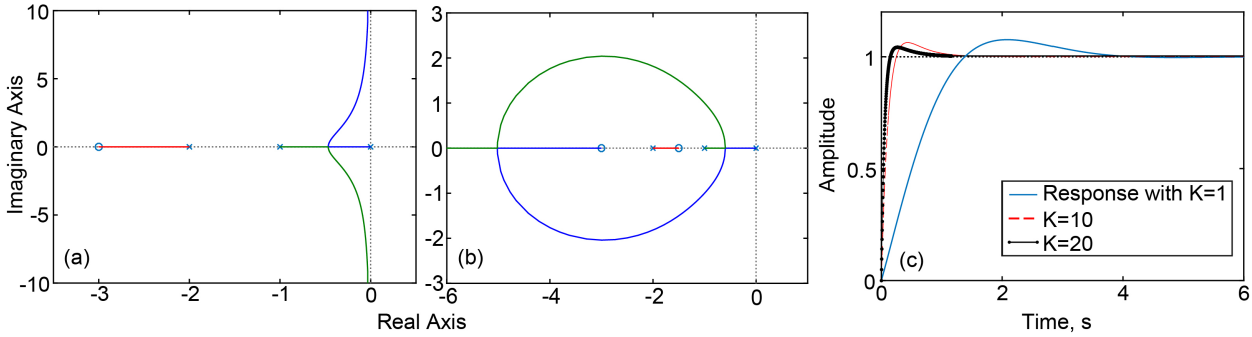

Figure 4.—(a) Root locus of a system with three poles and one zero to the left, (b) same three poles but with two zeros (one to the left), (c) response of the CL system with different proportional gains.

From Figure 3 it can be concluded that with two poles located on the real axis in the LHP and one zero located to the left of the poles, it is sufficient to bend the RL to the left as it would be desirable. If however, the OL system has three poles on the real axis in the LHP, one zero would not be enough to bend the RL to the left, as shown in Figure 4(a). If instead the zero was located between the rightmost two poles, the RL would look about the same as in Figure 4(a) shifted to the left, with the pole at the origin moving towards that zero. This can be seen by executing the following commands: **G=(s+0.5)/(s*(s+1)*(s+2)); rlocus(G)**. If two zeros are used to shape the RL for the case shown in Figure 4(a), with one zero located to the left of the poles and the other located between the leftmost poles, the RL shown in Figure 4(b) is obtained. This RL shape is desirable, because for any value of the proportional gain, the feedback system will remain stable. If two zeros are used again, but instead the leftmost zero is located between the two furthest left poles, the RL will look the same as in Figure 4(b), except that the circular trajectory would be more elongated in the vertical direction (try this with **G=(s+0.5)*(s+3)/(s*(s+1)*(s+2))**).

From this analysis, it can be concluded that a RL shape that bends to the left (as the gain, *K*, increases), in a circular like pattern as shown in Figure 4(b), is desirable. Also, to achieve this shape, the number of zeros required in the open TF are one less than the number of poles. Notice that in this example a pole is placed at the origin as a typical control system design would have for a step input command. The response of the feedback system with increasing OL proportional gains corresponding to RL points on the circular region shown in Figure 4(b), is shown in Figure 4(c). Notice that as expected from the RL in Figure 4(b), the system does not become less stable as the gain increases. In fact, in this case the system becomes more damped as the gain increases and as the RL moves closer to the real axis,

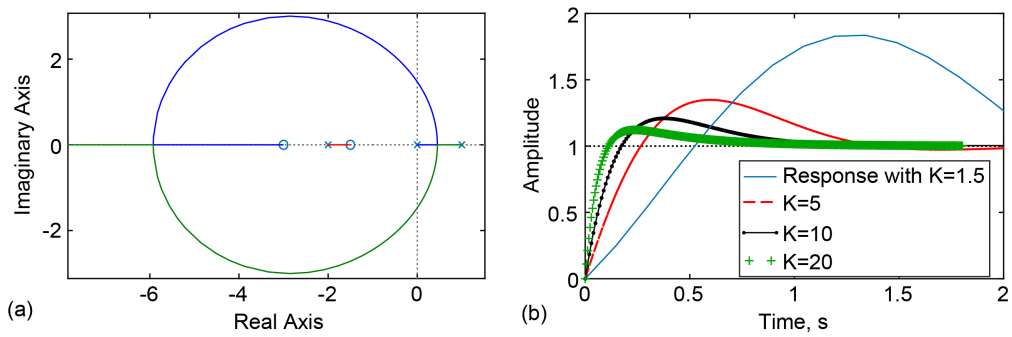

Figure 5.—(a) Root locus for the system shown in Figure 4(b), but with a pole in the RHP, (b) response of the CL system with different proportional gains.

while the response becomes faster. More design detail will be covered later about the response time and damping. The commands used for the feedback response are as follows:
G=((s+3)*(s+1.5))/(s*(s+1)*(s+2)); sys=feedback(G,1); step(sys); hold on;
G=10*((s+3)*(s+1.5))/(s*(s+1)*(s+2)); sys=feedback(G,1); step(sys,'r--'); hold on;
G=20*((s+3)*(s+1.5))/(s*(s+1)*(s+2)); sys=feedback(G,1); step(sys,'k.-');legend('Response with K=1','K=10','K=20').

Also, notice that in order to achieve the desirable RL shape shown in Figure 4(b), with two poles in the OL TF (the pole at the origin is a necessity for zero steady state error to step command), the placement of two zeros was necessary. If the controller design was to be restricted to a PI (Proportional Integral) control, this RL shape would not be possible, since PI control has one zero and one pole at the origin. If instead, PID control were to be used (two zeros and one pole at the origin), this RL shape would be achievable. However, it could be easily concluded that for an OL TF with at least three poles more than the number of zeros, even a PID control design that is well adjusted would not be able to achieve the desirable loop shape shown in Figure 4(b).

What if instead, one of the poles in the system depicted in Figure 4 lies on the real axis in the RHP? The shape of the root locus will be about the same as that shown in Figure 4(b); see Figure 5(a). As described before for such a case, the gain, *K*, would need to be above a minimum value for the system to become stable; see Figure 5(b). The question may be raised of what the RL will be like for the TF *G*, if it had a zero in the RHP. This case is beyond the scope of this discussion, since such a system would be non-minimum phase, whose control bandwidth would be fundamentally limited. What if the two poles were instead, a conjugate pair (complex poles always come in conjugate pairs)? Even in this case the shape of the RL would be about the same in terms of the circular pattern bending towards the left (see Figure 6(a)). For this OL TF, the MATLAB® command used to define it is **G=((s+3)*(s+1.5))/(s*(s+1+i)*(s+1-i)).** Figure 6(b) shows the feedback response of this system for different values of proportional gain. For small values of gain, this system is a little more underdamped compared to that in Figure 4, because the RL initially bends further away from the real axis.

As can be seen so far, the RL comes back on the real axis somewhere to the left of the leftmost zero. Therefore, it can be concluded that the placement of the leftmost zero has a substantial influence on how far the RL can be bent to the left, which influences how high the potential bandwidth of the system or how fast the system response can be (more on that later). In the examples shown, this zero is placed to the left (higher in frequency) of all the poles, but it can also be placed to the right of the leftmost pole. The placement of the lowest frequency zero (if placed properly) can affect the settling time and provide for composite natural frequencies. This however, will be covered in the Loop Shaping control design section.

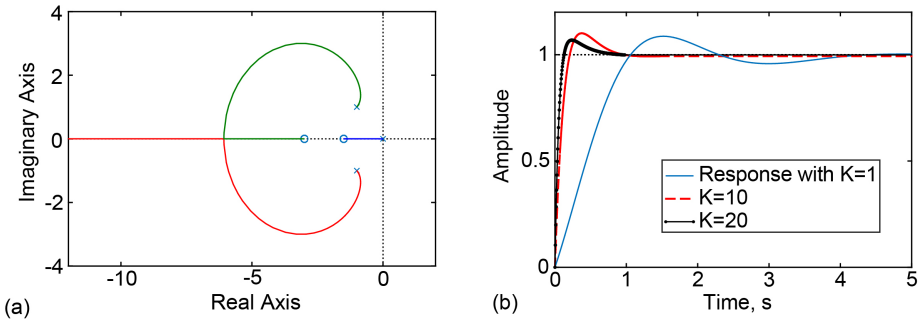

Figure 6.—(a) Root locus of a system with three poles (two conjugate) and two zeros to the left, (b) response of the CL system with different proportional gains.

2.2 Root Locus Control Design Comparison Example Using this Methodology and Additional Design Considerations

Without getting into the mathematical details of the RL theory, the discussions so far established a pattern or methodology by which more complicated control design problems can be approached. Consider a plant with the following TF $\boldsymbol{G_p(s) = 10/((s+30)(s^2+30s+709))}$, and with the following design specifications: The bandwidth, ω_c, of the control system design should be limited to 100 rad/s or up to 100 units/s speed for a unit step command. The steady state error to a step input should be zero. The Phase Margin (PM) should be greater or equal to 50°, and the Gain Margin (GM) should be greater or equal to 10 dB, with an overshoot of less than 20%. The noise amplitude at mid-frequency should be reduced to 0.1 or less (i.e., the OL TF should have a mid-frequency gain of at least 20 dB or 17 dB gain at $0.1\omega_c$). The settling time (t_s) or 98% of the response should be achieved in less or equal to 0.3 s.

The reason the bandwidth or the response time of the system is limited is because physical processes and actuation systems have rate limits, whether physical or operational, that limit how fast these systems can be driven. If a control designer takes advantage of the bandwidth of the control system, benefits can be realized in terms of the control system performance for speed and disturbance rejection. If a rate limit is prescribed in the control system design, this can also be used to appropriately limit the bandwidth of the control system in order to allow linear operation and a more predictable control system behavior.

Figure 7(a) shows the RL for the TF of just the plant (controller TF=1), and Figure 7(b) shows the RL with an integrator added for the controller, which is a necessity for zero steady state error. The grid rays signify constant damping. The semi-circles centered at the origin show the frequency of the complex poles of the CL system, if the gain is selected such that the poles of the CL system intersect these semi-circles. The damping of the CL system can also be computed for a selected proportional gain (a point on the RL) by vectorially simplifying the CL TF (as discussed before) and reducing it into a dominant pair of complex poles. Then the damping ratio, ζ, is the magnitude of the real part over the respective frequency ω_n. The dominant or natural frequency of the CL system in rad, ω_c, is the frequency at which the magnitude of G in the denominator (1+G) of the CL TF goes to 1.

As shown in Figure 7(b), adding a pole at the origin causes the poles to come together as the gain increases and then split towards +/- ∞. Due to the design specs for the overshoot and for the bandwidth or speed of the system, a choice of $\zeta = 0.8$ and $\omega_c = 100$ rad is selected (see Ref. 2 for selecting ω_c for the speed of the system) to show the limits of the control system if just an integrator were chosen for the controller. Using the command **sgrid(0.8,100)**, a grid is created in Figure 7(b) showing the rays of 0.8 damping and 100 rad/s control system bandwidth. The RL trajectory comes close to this point. So this performance is achievable, if the gain is selected to locate the roots at this point (which will be shown

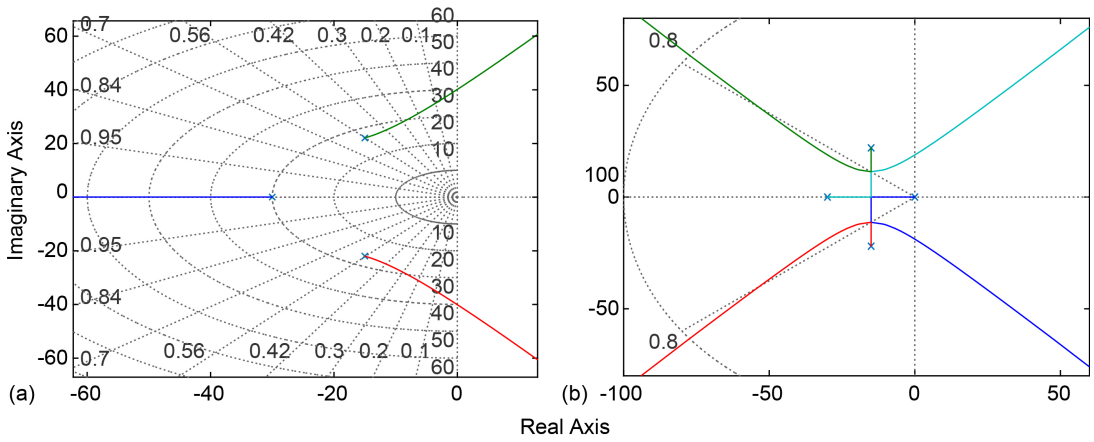

Figure 7.—(a) Root Locus of the TF of just the plant, (b) Root Locus of the TF of the plant and an integrator.

shortly). Except that such a point (with the same gain), also exists on the RL shown in the RHP, which will cause the system to be unstable (even for smaller gain). Thus, let's revert back to the methodology considerations previously discussed in order to design a feedback controller for this system to satisfy the specifications and achieve good performance.

From Figure 7(b) it can be seen that the OL TF for this system so far has four poles at s1=0, s2,3=-15+/-22i, s4=-30. Similar to the RL shown in Figure 4(b) or Figure 5(a), it would be desirable to properly place the leftmost zero on the real axis to cause two of the poles to loop towards the left, break in to the real axis, with one of the poles moving to the zero, while the other goes towards a zero at -∞. For the other two poles (the poles on the real axis), the strategy is to place two zeros nearby (preferably on the real axis) to cause these poles to move towards the zeros. Placing the leftmost zero somewhere to the left of the pole at s=30 will be a necessity in this case, in order to meet the 100 rad/s bandwidth specification or 100 units/s speed, with sufficient damping to also meet the overshoot specification. Unless break-out and break-in calculations are performed using RL theory, the placement of this zero involves some trial and error in order for the break-in of the poles into the real axis to occur somewhat close to 100 rad/s. As mentioned before, the placement of the lowest frequency zero can impact the settling time. Without involving calculations (see Ref. 2 for more detail), the lowest frequency zero is placed at s=-20, and the next zero is placed at s=-25 (i.e., between the lowest frequency zero and the pole frequency at s=-30. However, if the settling time specification is not met, the first zero can also be adjusted by some trial and error.

Based on this approach or design considerations, the zero frequencies are selected at s_{z1}=-20, s_{z2}=-25, and s_{z3}=-55, which results in the following OL TF, $\mathbf{G(s) = K[(s+20)(s+25)(s+55)]/[s(s+30)(s^2+30s+709)]}$. The RL of this design is shown in Figure 8(a), together with its **sgrid** in MATLAB® of 0.75 damping and a CL complex pair pole frequency, ω=100 rad/s. Figure 8(b) shows a display of the MATLAB® figure where the + button is used to place a cursor point at about the intersection of the 0.75 damping ray with the RL trajectory. This cursor point displays the OL TF proportional gain at that point of *K*=109, it shows the CL complex poles, and actual damping of 0.772, the overshoot, and a complex (conjugate pair) pole frequency of 80.9 rad/s. Note that if the time response of the CL system does not agree with what is expected from this selection, it is because there exists another point on the RL trajectory with the same gain at a lower frequency which overtakes or dominates the response.

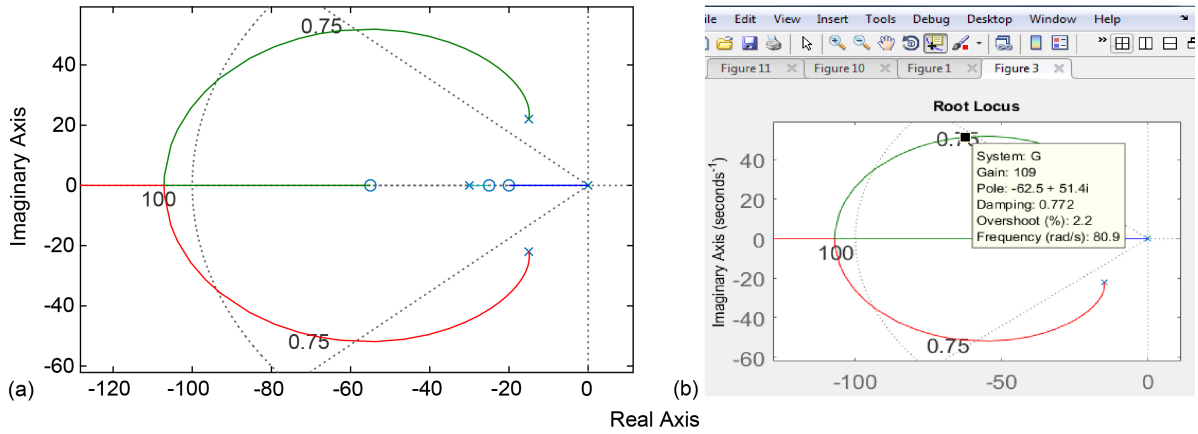

Figure 8.—(a) Root Locus of the TF of the design example, (b) MATLAB® figure showing the Root Locus of the same system with the cursor point for the selected location of the CL poles.

The resulting natural frequency of the complex poles in this design, ω_n, is less than 100 rad/s, but the resulting crossover frequency, ω_c needs to be checked with a bode plot to see what the actual bandwidth or crossover frequency of this design would be. The crossover frequency is the frequency where the bode plot crosses the 0 dB magnitude, and here the crossover frequency and the bandwidth of the system are defined to be the same, as the system can respond to disturbances up to the crossover frequency. The value of the crossover frequency in rad/s is also the initial speed of the system in units/s (see Ref. 2). Adjusting the frequency of the leftmost zero, however, will allow the RL trajectory to break-in more to the right for smaller values (frequency) of this zero, or more to the left for larger values. This allows both a desirable damping if necessary (pole location closer to real axis for higher damping) and the complex pole pair frequency to be chosen at the same time, which influences the speed of the control system. Note that choosing a point on the existing RL, like in Figure 8, to the left of the ω=100 rad/s grid line, will make the system response faster. While choosing points inside the ζ=0.75 grid rays and closer to the real axis, will make the system response more damped.

The bode plot of this TF with a gain K=109 is shown in Figure 9. It is produced using the command **bode(109*G); grid**. This figure can also be developed by hand by substituting $s = j\omega$ in the TF G and evaluating G for different values of frequency ω, and then plotting the magnitude and the phase angle point-by-point. For this gain or magnitude plotted in Figure 9, the crossover frequency exceeds the 100 rad/s limit placed by the specification. For a quick fix (without changing the OL TF and the RL design), zoom in on the bode plot at 100 rad/s and find out the magnitude at that point (dB $|_{100\ \text{rad/s}}$). Then perform the antilog, $x=10^{\text{dB}(100\text{rad/s})/20}$ in order to find the ratio of the gains that will provide for 0 crossing at 100 rad/s, and divide K=109 by this factor x. Following these steps, the resulting gain turns out to be K=84.9. Over-plotting the bode of the TF with this gain in Figure 9 shows that the bode with the revised gain indeed crosses at 100 rad/s. With the reduced gain, the RL pole location will move a little to the left from the previous location, and thus the resulting CL system would be expected to become a little less damped. If the resulting damping or overshoot would not be satisfactory, then the RL trajectory would need to be adjusted instead, by adjusting the location of the leftmost zero.

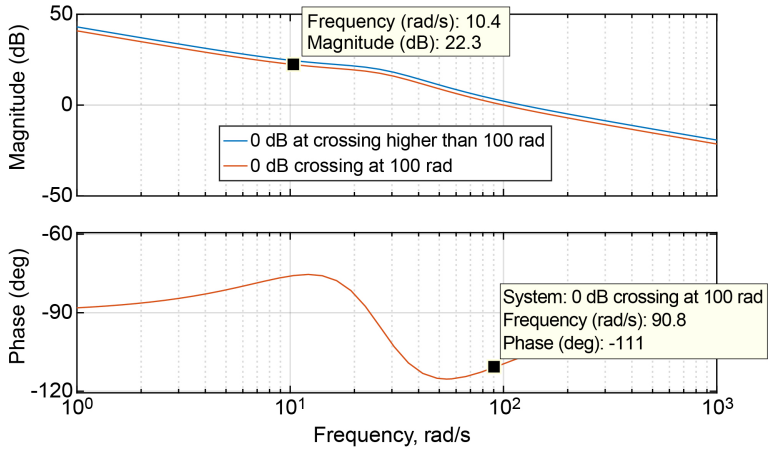

Figure 9.—Bode plot of the OL TF design.

From the cursor point on the phase portion of this bode plot, it can be seen that at about 91 rad/s (close to 100) the phase is -111°, with the phase ascending at that point. Thus, the stability PM of this design would be more than 180°-111° or 69°. Also, this design will have infinite GM (the phase doesn't cross -180°). So both the PM (50°), and the GM (10 dB) are met with this design. Also, the cursor point at 10 rad/s shows that the gain at that frequency is approximately 22.3 dB, which meets or exceeds the design specification at the mid-frequency range. The magnitude of the OL gain at a certain frequency before the crossover signifies the magnitude by which the control system attenuates disturbances at that frequency for disturbances coming into the system at the output of that plant. For instance, if the gain at a certain frequency is 26 dB, the controller will reduce disturbances at that frequency by a factor x, where $x=10^{(26/20)}=20$.

The next step is to show the time response of the CL system with the OL TF that was just designed, in order to evaluate if the control system design meets transient response specifications. For briefness, this will be done after the plant and the controller TF are separated in this OL design. If the plant TF is left alone as it should be, the controller TF due to this OL design will end-up with three zeros and one pole (the pole at the origin), which results in an improper TF. In order to make the controller TF proper and the overall OL TF proper or even strictly proper (more poles than zeros), it is necessary to pad the controller TF with at least two poles, and do so without significantly affecting the design that has been obtained so far. To accomplish this, the poles are added here at10x the crossover frequency or a little higher. This way, the effect of these poles on the phase of the OL TF or the PM will be about gone near the crossover frequency. Note poles or zeros have an effect on the phase of the OL TF, starting at 0.1x their placement frequency and the effect ends at 10x the placement frequency. Based on that, the choice here for the controller TF is $\mathbf{G_C} = [(\boldsymbol{84.9/10})(\boldsymbol{s+20})(\boldsymbol{s+25})(\boldsymbol{s+55})]/[\boldsymbol{s}(\boldsymbol{s/1000+1})(\boldsymbol{s/1100+1})]$. Notice that the poles are added in a normalized TF form, which does not change the gain of the controller or the gain of the OL TF. Also, notice that the controller proportional gain is divided by the gain of the plant, so that the resulting OL proportional gain remains the same as the one designed (i.e., K=84.9).

First, let's check if the bode plot of the designed OL TF and the corresponding OL TF with the padded controller match, at least up to and a little beyond the crossover frequency, which will ensure that the designed performance or specifications are not compromised. Figure 10 shows the bode plot of the designed OL TF and that with the padded controller. Their bode magnitudes overlap and continue to overlap well after the crossover frequency. The phase of the padded controller at the crossover frequency (100 rad/s) is reduced from approximately -109° to -120°, but the stability PM of the CL system with the padded controller TF at 60° still meets and exceeds the design specification. As seen in this figure, the phase of the OL TF with the padded controller crosses 180°, and at that frequency the gain is

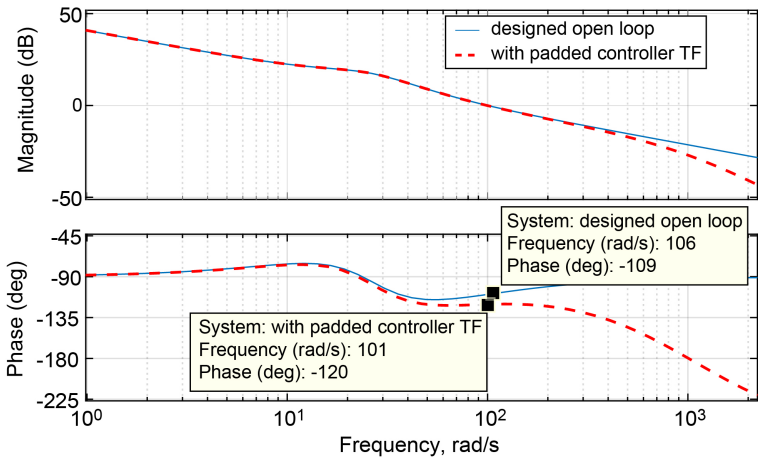

Figure 10.—Bode plot of the OL TFs of the designed and that with the padded controller.

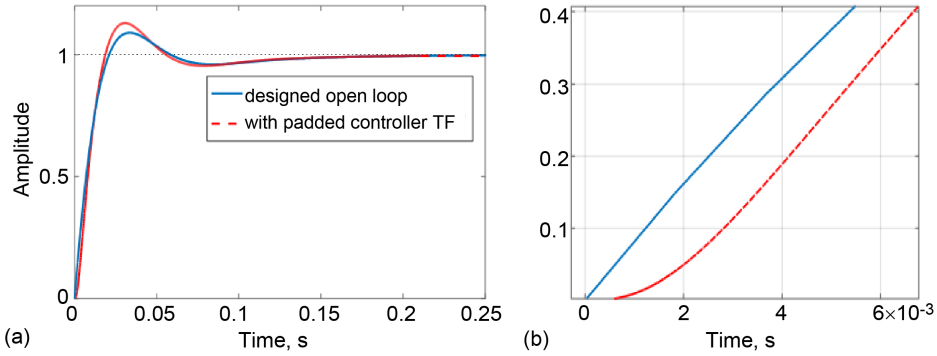

Figure 11.—(a) Response time of the CL TFs of the designed and that with the padded controller, (b) their initial response time.

approximately -27 dB (not shown), which provides for a stability GM of 27 dB. This GM also well exceeds the design specification of 10 dB. To reduce or eliminate any effect due to the padded poles in the controller TF, their frequencies can be increased accordingly. Note, however that the sampling time that would be required to resolve the highest frequencies in the design and for continuous time system simulation would be reduced accordingly.

The unit step response time of the feedback system without and with the padded controller design is shown in Figure 11(a). The settling time (98% of response) in 0.3 s is also well met with this design. Figure 11(b) shows their corresponding initial response times. The initial response time or the highest speed of the feedback system with the padded controller (after some initial delay) is approximately 80 units/s, which is close to the 100 units/s limit in the specifications. This RL design is a little underdamped. However, by repositioning the leftmost zero to permit increased damping at the RL selected point for the pole location, all the design specifications can be met and the designer could also achieve a more damped response than that shown in Figure 11(a). A more damped response can also be achieved by properly positioning the lowest frequency zero, but this will be covered in the loop shaping section.

The RL design with the padded controller poles is shown in Figure 12. The inset shows a zoom-in of the RL region at low frequency. Comparing this low frequency region to the RL in Figure 8(a) shows that the original RL design remains about the same. However, the additional poles cause the RL trajectory to bend and cross into the RHP. Unlike the OL RL design shown in Figure 8, the padded poles cause the

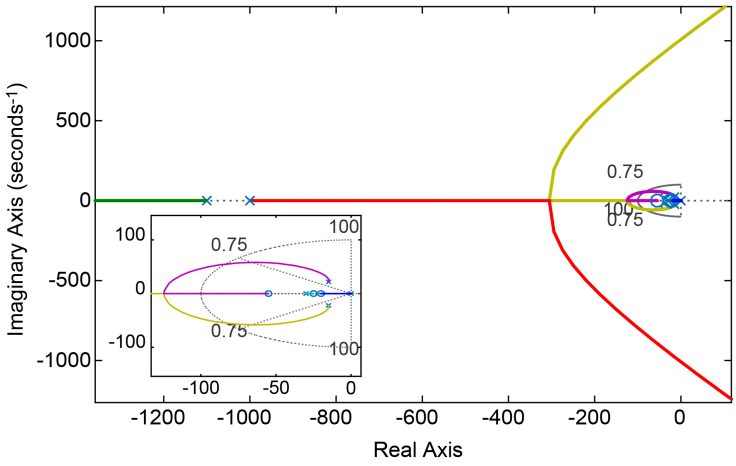

Figure 12.—Root locus of the OL TF with the padded controller design.

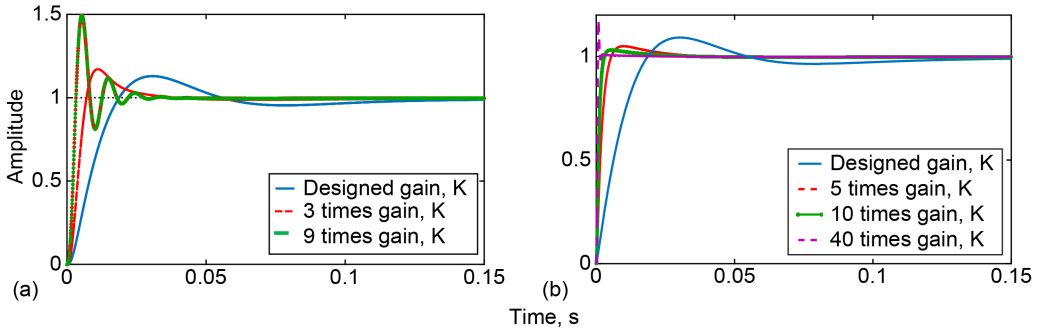

Figure 13.—Step response of CL system for different proportional gains with padded controller poles located approximately (a) 10x crossover frequency, (b) 100x crossover frequency.

pole at s=1000 and one of the complex poles to come together and split to cross into the RH plane as shown in Figure 12. The step response without the padded poles, for increasing proportional gain, would look similar to the response shown in Figure 6(b), but the step response with the padded poles is as shown in Figure 13(a). The proportional gain, *K*, for the OL TF is 84.9 (as previously designed) or 84.9/10 for the proportional gain of the controller TF. If the padded poles are placed higher in frequency, the difference in proportional gain that it will take to make the system unstable will increase as well. To demonstrate this effect, the step response in Figure 13(b) shows what happens as the gain increases, if the padded poles had instead been placed at approximately 10x higher in frequency or 100 times higher than the crossover frequency. This figure shows that as the proportional gain increases, the step response becomes faster, but more damped. This behavior continues until the gain increases close to 40x the original gain, at which point the response starts to become more underdamped. This design has robustness to high variability in the control system gain, as well as robustness to high uncertainty in plant pole zero locations. If the increased speed or rate of the system becomes problematic, rate limiting can be employed in the controller design. It is possible that the OL TF can be designed without the padded poles as initially shown in this example, and the response type shown in Figure 6(b) can be achieved, which can result in an inherently robust or ultra-stable control system design. This will necessitate a tightly integrated controller and plant design as shown in Appendix A.

Note that in this design example the rate of the control system output was limited. If instead, the rate of the control input to the plant or the actuator output was limited in the specs, then the rate of the plant

input could be checked to ensure that this rate is not exceeded while the output of the plant is driven at the highest rate prescribed. Alternatively, the actuator can be designed as a feedback system on its own, where instead its output rate is designed to be limited as described in this section.

The following are some general considerations for a RL design. If the complex pole pair frequency of the CL system TF is 1/8 or less than that of the rest of the poles and zeros, the CL system step response will be dominated by the second order polynomial of this complex pole pair. In such case, the settling time of the CL system will be approximately $4/(\zeta\omega_n)$, one time constant will be $1/(\zeta\omega_n)$, and the rise time (i.e., the time it takes to first get to or cross the steady state point) is approximately $1.8/\omega_n$. Even in cases where the frequencies of the CL TF are closer together, these approximations could still provide for a start to make subsequent adjustments as necessary in order to decide on the RL location, like the one shown in Figure 8(b). For instance, for a RL point selected as shown in Figure 8(b), the damping and the frequency (ω_n) can be used to quickly check if these values have a reasonable chance to meet such specs, before the feedback system is calculated and the step response is evaluated. Once the CL TF is generated using the gain shown by the cursor point in Figure 8(b), the roots of the numerator or the denominator polynomials can be computed by using the command **roots([a b c . .])**, where a, b, c …are the coefficients of the numerator or denominator polynomial, and where these coefficients are listed in descending order starting with the coefficient of the highest power of *s*. Notice that for a given RL, multiple RL branches may exist, which may give rise to multiple real poles or to more than one complex pole pair for the same proportional gain value. In such cases, the poles or the pole pairs that dominate the response are the low frequency ones, or the marginally stable or the unstable poles, if they exist.

This concludes the RL design methodology covered in the paper, which is relatively simple to master, and it can be used to expedite the RL control design process without necessarily the need to understand the details of RL theory. In general RL is a powerful way to achieve control designs that are at least as good as any other classical control design technique.

3.0 Loop Shaping Design Approach

The loop shaping approach presented in this paper is covered in detail in Reference 2, and an application of this design approach is provided in Reference 3. Here a controls design is carried out for the example in the previous section based on this LS approach. The design process is the same as that discussed in these references, except for some design considerations that will be included here in order to further simplify and expedite the design process. How well the approach satisfies the specification in this design example can be compared to the RL method covered in the previous section. However, the design approach presented here is not necessarily better than the RL method, since a controls design that can be achieved with RL only depends on the skills of the controls design engineer. What this loop shaping controls design approach brings forth is that this is another approach to achieve a very good controls design, and as will be seen, this method may be easier to utilize than the RL. Yet, this LS method identifies some additional controls design considerations that can also be utilized in the RL design approach.

In loop shaping design, usually one converts time domain specs like percent overshoot, steady error, noise rejection and settling time into frequency domain requirements for the target loop shape $G_C(s)G_P(s)$. Some rule of thumb relations are often used in this process to find required PM, low and high frequency slopes for magnitude and crossover frequency, etc. (Ref. 4). While these rules of thumb can be useful, the approach covered here is somewhat different in that the only specification utilized for the loop shaping is the speed of the actuator or the desired rise time, which also sets the crossover frequency and the settling time. The rest of the specifications are not considered initially, as the approach here is to maximize

control system performance in terms of adequate stability and disturbance rejection (Ref. 2), with very low overshoot if any. The amount of overshoot allowed is typically specified in a design. However, there is no advantage to have any significant overshoot as it also adversely affects control system robustness. As such, low stability margins or any significant underdamped response would only be considered to be necessary if there are competing requirements, such as higher than normal disturbance rejection, for instance, higher than 20 dB at 0.1 times the crossover frequency, ω_c (see Ref. 2).

3.1 Loop Shaping Design Methodology Considerations

The LS shape approach is also based on designing or shaping the OL TF of the control system. Unlike the RL approach, however, this is done independently of the plant TF and based on information about the speed or desired speed/rate limitation of the process, and the rest of the control design specifications. Then once the desired OL shape that satisfies the specifications is achieved, the controller is designed using the plant information, so that the resulting OL TF matches the desired one. The design of the desired OL TF is done with certain considerations that enhance the stability properties and overall performance of the control system.

The design procedure is as follows (see Ref. 2 for more detail). First the desired OL TF, $G_d(s)$ is designed, based on the speed specification or speed limit of the process or its actuation system. For this, a pole is placed at 1/10th the frequency of this limit of units/s or rad/s; a zero is placed somewhere preferably between 1/4th and ½ the pole frequency; a pole is placed at the origin as before; and the gain G_d is calculated so that at the mid-frequency range (i.e., at the frequency range between the zero and the higher frequency pole) the gain is 10 or 20 dB in logarithmic scale.

In summation, the reasoning for these selections for G_d is as follows (Ref. 2). The gain of 20 dB at mid-frequency will help to maintain high disturbance rejection for the feedback control system; about as good as it can be achieved (Ref. 2) while also maintaining a reasonable PM for stability. With a gain of 20 dB at the mid-frequency range, the location of the pole at 1/10th the speed of the system in rad/s (the speed in rad/s is the same as the crossover frequency or bandwidth of the system) will allow the gain to attenuate by -20 dB/decade and reach 0 dB at the desired crossover frequency. With a pole at the origin for zero steady-state error, the zero is needed in order to flatten the gain and maintain it at 20 dB at the mid-frequency range. The zero also serves a couple of additional purposes. It helps to boost the phase to help with the PM for stability. Also, the frequency range of its placement allows the CL system response time to have composite dominant frequencies (Ref. 2) whereby the initial portion of the response is second order type and its time constant ($1/\omega_c$) is due to the crossover frequency, and whereby the response near the settling portion becomes first order with a time constant that is due to the frequency of the zero, ω_z. A first order response near the settling portion of the system response is desirable, because a first order type response is by definition a damped response. This further aids in the stability and robustness of the control system design.

Say that the speed limit of a certain plant is given to be 200 units/s or 200 rad/s. Based on these design guidelines, the desired OL TF, G_d, would be $\boldsymbol{G_d = 10*\omega_z (s/\omega_z +1)/[s(s/20+1)]}$ in normalized form, with ω_z selected to be between 5 and 10 rad/s for this case , which gives the gain value required for 20 dB gain at mid-frequency. Alternatively, in standardized TF form $\boldsymbol{G_d = 10\omega_p (s +\omega_z)/[s(s+\omega_p)]}$. For such a design, let's see what the step response of the CL system looks like, as well as the bode plot of the OL TF, G_d. The zoomed in step responses in Figure 14 show that for all the 4 cases, the CL system response near the settling time is first order type due to the placement of the zeros. Figure 14 also shows that for the zero at 2.5 rad/s (1/8th of the pole at 20 rad/s), the system takes a relatively long time to settle. For the

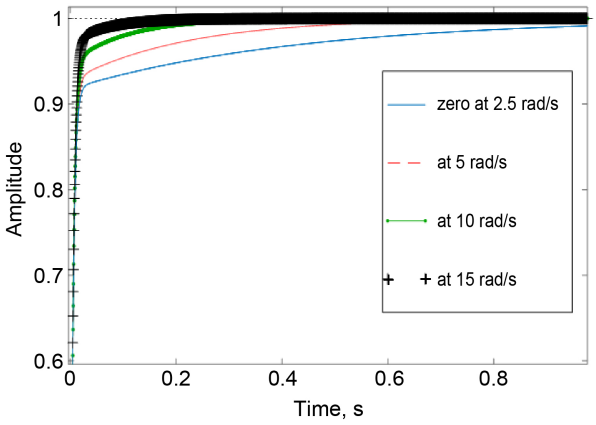

Figure 14.—Response of the CL system for different zero frequencies of the desired OL TF, G_d.

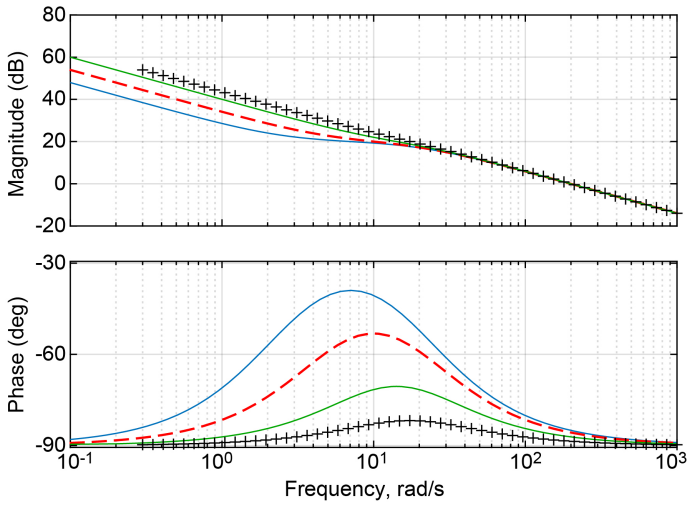

Figure 15.—Bode plot of the OL system G_d for different zero frequencies.

zero at 15 rad/s, the system settles relative quickly, but if system robustness was important, there would be more chance for this system to become underdamped if the dynamics of the plant change or the OL TF changes significantly. This is because the initial response, which is second order, takes the step response of the system almost to the set point, which increases the chances that the system response can become underdamped if the dynamics of the plant change. Arguably, the range of zero placement between 1/4th and ½ the frequency of this pole (i.e., between 5 and 10 rad/s for this case), compromises between settling time and system robustness.

For the same cases, Figure 15 shows the bode plot of the desired OL system design, G_d. It shows that the crossover occurs at 200 rad/s for all cases as designed, and also that the mid frequency gain is 20 dB for all cases as was also intended. Notice the mid-frequency range (the frequency range between the zero and the pole) is different for each of the cases. This figure also shows that the stability PM is about 90° for all cases (more than adequate), while the GM is infinite (i.e. the phase does not cross -180°).

The next step is to design the controller TF, with knowledge of the plant and Gd. Since the only unknown is the controller TF G_C, this involves a calculation, as $G_C=G_d/G_P$, or in logarithmic scale $G_C=G_d-G_P$. However, due to the vector math involved, this is not a simple calculation to perform to calculate the gain, poles, and zeros of the controller TF. Therefore, a more simplified approach will be carried out in

this paper in order to expedite the design process, and find the controller TF for which the resulting OL bode will match that of the desired OL TF, G_d. For the sake of briefness, this approach to synthesize the controller TF, so that the designed OL gain vs. frequency of the control system matches that of the desired one, will be demonstrated in the next section using the example problem from the previous section.

3.2 Loop Shaping Methodology Example and Additional Design Considerations

For the example plant given in the Root Locus section, $\boldsymbol{G_p(s) = 10/(s+30)(s^2+30s+709)}$, and for the specifications provided (i.e., ω_c =100 rad/s, zero ss error, PM ≥50°, GM≥10dB, over shoot < 20%, noise reduction 17 dB at 1/10 ω_c, $t_s \leq 0.3$ s), the desired CL TF will be $\boldsymbol{G_d(s)= 50(s/5+1)/[s(s/10+1)]}$, based on the approach discussed in the previous section. Notice that the frequency of the zero was chosen in the upper range in the guidelines provided in the previous section, but this could be adjusted if desired as long as the settling time spec is met. Figure 16 shows the bode plot of the OL TF, G_d, which shows that the crossover occurs at 100 rad/s as per the spec, at 10 rad/s the gain is approximately 17 dB which meets the spec, and that the PM is about 90° with infinite GM (more than meets the specs). Figure 17 shows the step response of the CL control system with the desired OL TF, G_d design. The figure shows the composite natural frequencies of the response discussed in the previous section, the settling time specification which is met with this design, and the inset that shows the initial response or speed of the system, which turns out to be approximately 85 units/s (close to the limit of 100 units/s).

To calculate or synthesize the controller TF in order for the actual OL TF of the control system to match the desired OL TF, the first thing that needs to be done is to normalize the plant TF in order to extract its normalized or its low frequency, so called, DC gain. Given the plant TF above, this normalization is performed as $\boldsymbol{Gp(s) = \frac{10}{30(709)} \frac{1}{(s/30+1)(s^2/709+\left(\frac{30}{709}\right)s+1)}}$, where the DC gain of the plant, K_P=10/(30×709)= 4.7×10^{-4}. Then the gain of the controller TF, K_C, can be calculated knowing that the actual or designed DC gain for the OL TF needs to match that of the desired OL TF, as $K_d = K_C K_P$, and for this case K_C=50/4.7×10^{-4}=1.063×10^5. The next step is to match these OL gains in the frequency domain by inspection, starting from low and proceeding towards higher frequencies. The simplest way to accomplish this task is to keep the poles and zeros of the G_d and cancel the poles and zeros of the plant. From before, the plant has poles at s1,2=-15+/-22i (ω_n =26.6), and s3=-30 rad/s. Based on that, the

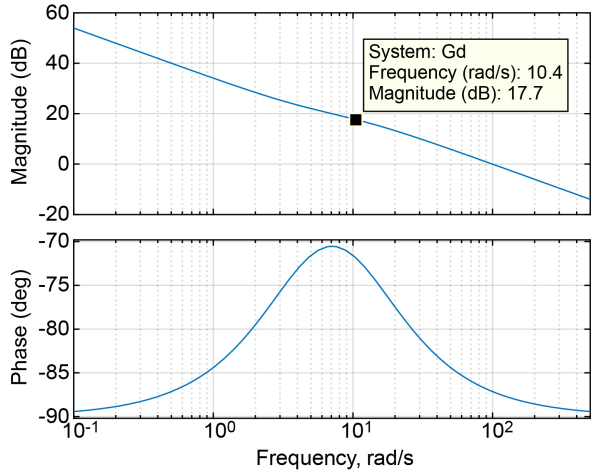

Figure 16.—Bode plot of the OL TF design, G_d, using Loop Shaping.

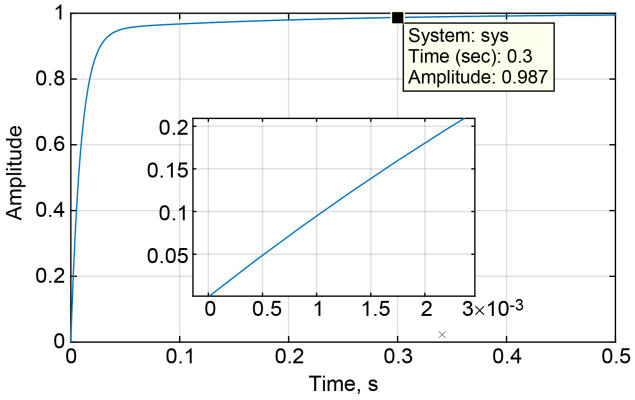

Figure 17.—Step response of the CL system with the desired OL TF design, G_d, using Loop Shaping.

controller TF can be synthesized as $Gc1(s) = 1.063 \times 10^5 \frac{(\mathbf{s/5+1})(\mathbf{s/24.6+1})(\mathbf{s/28.6+1})(\mathbf{s/30+1})}{\mathbf{s(s/10+1)(s/1100+1)(s/1300+1)(s/1500+1)}}$. Notice that in order to try to cancel the effect of the complex poles of the plant, zeros have been placed at 24.6 and 28.6 rad/s on the real axis, within +/- 2 rad/s of the complex poles natural frequency. If the double pole was on the real axis, the placement of the zeros on either side of the double pole would better compensate in case the precise frequency of the double pole is not known or if it shifts. For the complex conjugate poles in this case however, the further out to the left the zeros are placed, the further out the poles will travel on the RL before they come back to the real axis, and therefore the higher the permissible dominant frequency or bandwidth of the control system design. Thus in this case for the complex poles, the placement of these two zeros, along with the placement of the leftmost zero, also drives the allowable bandwidth of the system. Notice that padding poles have been inserted as before at 1100, 1300, and 1500 rad/s in order to make the controller TF proper (in this case strictly proper, but it could also be just proper). Alternatively and as the case may be, direct cancelation of the plant frequencies can also be performed, in which case the controller TF in standardized form would be $Gc2(s) = K\frac{(\mathbf{s/5+1})(\mathbf{s+30})(\mathbf{s^2+30s+709})}{\mathbf{s(s/10+1)(s/1100+1)(s/1300+1)}}$, where in this case K=K_d/K_{ps}=5, and K_d and K_{ps} are the proportional gains of the desired and the standardized plant TFs, respectively. Notice that the padding poles are added in normalized TF form, so that the gain of the controller is not affected by this addition. Notice also that in this case a just proper TF is chosen for the controller, but it could be instead selected to be strictly proper.

Another approach to develop a controller TF for LS control design will be covered in an example provided in Appendix C for a more involved control design process, which also serves to reinforce some of the control design concepts discussed in this paper.

The bode plot of the desired OL gain and the actual OL gain for both controller designs is shown in Figure 18. The OL gain with controller *G*c1 has a bump because of the complex pole in the plant. Had the OL gain with controller *G*c1, exactly matched that of the desired OL gain design, the step responses of their respective CL systems would be exactly matched. On the other hand, the desired OL gain as shown in Figure 18 precisely matches with that of the controller *G*c2 at the lower frequency range that extends well beyond the crossover frequency, which will cause their respective step responses to match. Figure 18 also shows that for the control design *G*c1, the PM decreases to approximately 67° (but more than exceeds the spec), while for controller *G*c2 the PM is about the same as the desired one. Their respective GMs are about 20 to 30 dB, which also exceed the spec. Step responses of the desired control system and the CL system with controller *G*c1 are shown in Figure 19. The response with controller Gc2 is not shown in Figure 19, because that coincides with the desired one, and cannot be discerned in this figure. The responses with ether controller *G*c1 or *G*c2 still exhibit a first order type response near the settling, which is desirable for enhanced stability and robustness. The speed or initial response of the system as well as the settling time remain about the same as that shown in Figure 17.

Figure 20 shows the tolerance or robustness of the LS control design to gain variability, starting from the original gain (K=1) and up to 10 times that. The stability of the LS design is aided by the composite natural frequencies, with the first order type response near settling. This is evident from the response of 10 times the original gain, which shows that after the initial overshoot the response quickly settles down. The loop shape control design as covered here, also has significant tolerance to variability in system dynamics such as pole zero locations. If this LS control design is implemented as a model following control system as shown in Appendix B, with the reference model, G_r(s), being the feedback system of the desired OL TF, G_d(s) (i.e., **Gref=feedback(Gd,1)** in MATLAB®) and with the external feedback gain set to 1, the control system response for K=1 to K=10 would be about the same as that shown in Figure 20 for K=1 (see Appendix B). That is, significantly more robustness would be achieved with LS control integrated into a model following control design.

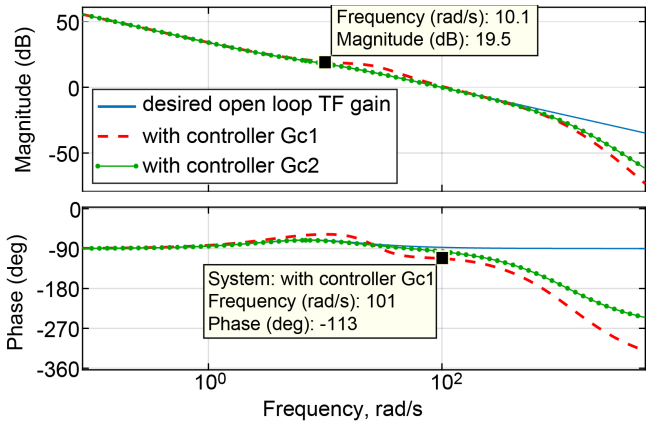

Figure 18.—Bode plot of the desired OL TF design, G_d vs. the actual open TF based on the controller design.

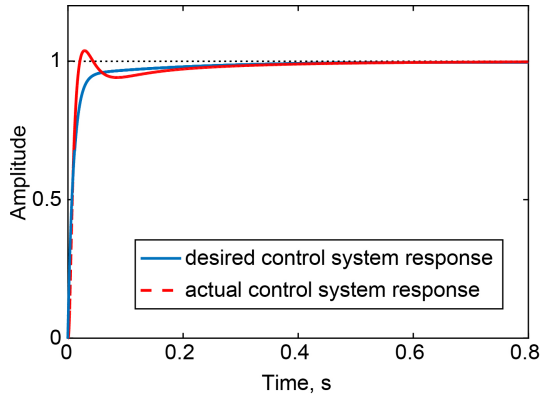

Figure 19.—CL system step responses of the desired and the actual system design with controller *G*c1.

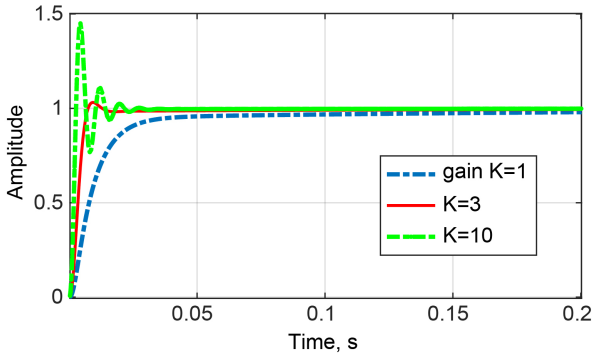

Figure 20.—Response time of the LS control system for controller *G*c2 with the original gain (K=1), and up to 10 times the original gain.

The RL of the LS control design in this example with controller *G*c2, zooming in the low frequency region, is shown in Figure 21. Here the LS design ends up with a RL similar to that obtained with the RL design shown in Figure 8. Increasing the gain in this LS design results in the same step responses shown in Figure 20, and increasing the frequency where the padded poles are placed would have the same effect as that shown in Figure 13(b).

In the RL design section it was mentioned that the lowest frequency zero can influence the response time and allow the CL system step to exhibit a first order type response near the settling time. This guideline originated from the LS methodology (Ref. 2) and is elaborated on in this section. However, this guideline can also be applied to the RL approach to potentially improve the control system design. To demonstrate this effect with the RL control design, the lowest frequency zero in that design, at s=20 rad/s, was moved to 5 rad/s (everything else remaining the same). The effect of this change in the CL step response of the RL control design is shown in Figure 22, which can be compared to Figure 11. This particular design does not meet the settling time spec of 0.3 s, but the objective here is to demonstrate that this type of response that aides the stability and robustness of the system is possible even with RL. Figure 23 shows the shape of the RL with the modified RL design, which remains basically the same as that of the original design shown in Figure 8.

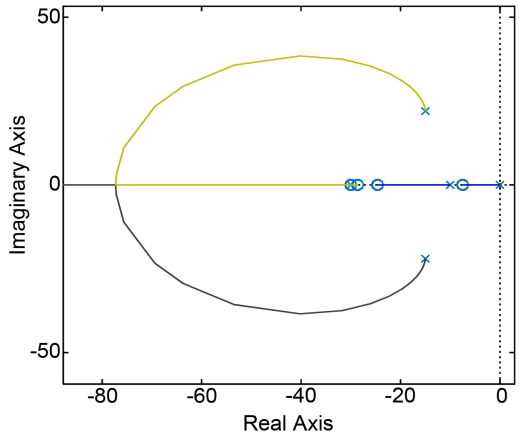

Figure 21.—Root Locus of the loop shape design zooming in the low frequency region.

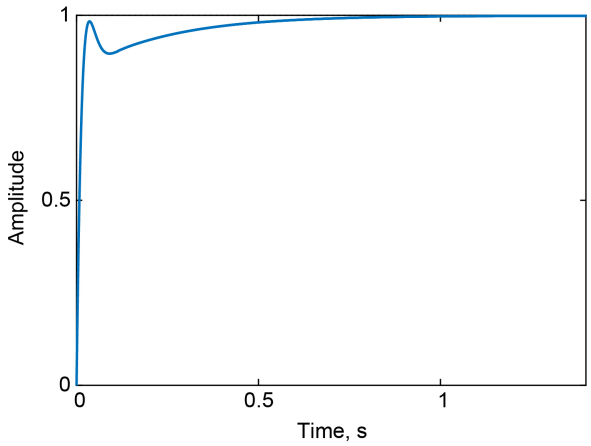

Figure 22.—Step response of the modified RL design in the previous section that shows the effect of relocating the low frequency zero from 20 to 5 rad/s.

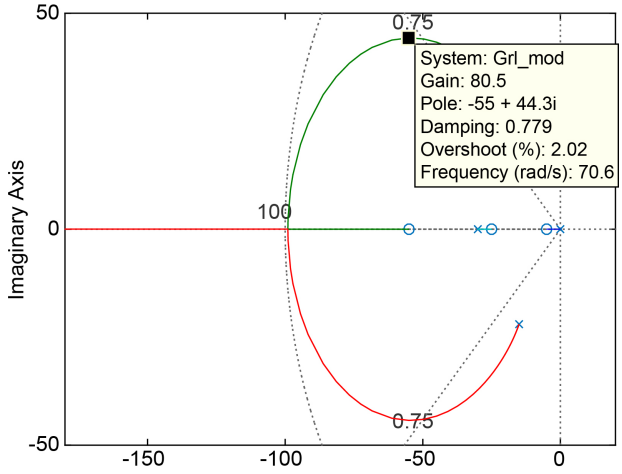

Figure 23.—Root locus of the modified RL design.

The padded controller TF in this modified RL design shown in Figure 23 is made to be strictly proper, even though that does not need to be the case and in fact, its corresponding RL design may in general end up being more robust without the additional pole. Many times control designers insert a pole at a slightly higher frequency than the crossover frequency in order to cause the gain to roll-off at a higher rate than -20 dB/dec and to prevent the possibility of an unmodeled zero at this frequency range to cause stability problems. Such designs however, that can compensate for a potentially unmodeled zero at frequencies slightly higher than the crossover frequency must be used judiciously. If such a zero does not exist, the addition of a pole, if it makes the controller TF strictly proper, can adversely affect performance or robustness as has been previously discussed.

There are cases such as in commercial propulsion systems, where the response time of the control systems is required to be relatively slow compared to the speed of the actuation system. For such cases, it is possible to design the control system to be relatively slow as required, while still taking advantage of the speed of the actuator to improve system performance. This is covered in Appendix B.

Some limited comparisons have been performed here about the ability between RL and LS control design techniques to achieve good performance or about as good performance as is possible with a classical controls system design. The RL and LS designs covered here achieve about as good performance

as possible. For a general idea of what is considered to be a good design, refer to Section 3.1, and for more explanations or quantitative information in this area, see Reference 2. Keeping in mind that both RL and LS control design approaches are classical lead-lag compensation techniques, general performance comparisons between these two control methods are more or less indicative of control design skills. Perhaps the use of LS may be a little easier or intuitive than RL, but even that is arguable as both control design approaches presented here are relatively easy to apply.

4.0 PID Control for the Design Example

A PID control design is in general ad hoc. Even though some methodical PID gain tuning control system design techniques exist, they are not suitable for all types of plant TF structures. This section, therefore, will not cover a particular PID gain tuning approach. Instead, the graphical tool available in MATLAB® for PID tuning will be utilized for the control problem presented in the previous sections, which with a little user skill is found to produce as good as or better designs than any of the existing PID tuning techniques.

If MATLAB® is used for PID design, this is an example of the process that is followed. The command **pidTuner(Gp,'pid')**, brings up the graphical tool. There is a "domain" choice for either the time or the frequency domain. In the frequency domain two sliders are provided, one for the PM (tuned to 50° per the spec in this example), the other for tuning the bandwidth. The bandwidth slider was started from a relatively high value, and was adjusted down until the step response time of the CL system (also displayed on this window) met the settling time spec of 0.3 s for 98% response.

The PID gains for this design, also displayed on this window, were Kp=3367, Ki=3.77×10^4, Kd=75.19. This results in the following PID controller TF **Gc=Ki*[(Kd/Ki)*s^2+(Kp/Ki)*s+1]/(s*(s/1000+1))**. Notice the pole at 1000 rad/s is a padding pole that was inserted afterwards to make the controller TF proper. The OL bode plot of the control system (**bode(Gc*Gp, {0.1,200})**) is shown in Figure 24. This figure shows that the crossover or the bandwidth of the control system is approximately 26.6 rad/s (actually in the MATLAB® window it showed 27.95 rad/s). This bandwidth is significantly less than that achievable with the RL or LS designs. With this low bandwidth, the design satisfies both the phase and the GM as seen in this figure. This figure also shows that the mid-frequency gain of approximately 20 dB (per the spec) is achieved at about 2 rad/s, and therefore, the PID design in this example will achieve significantly less disturbance rejection compared to the RL or LS designs covered earlier.

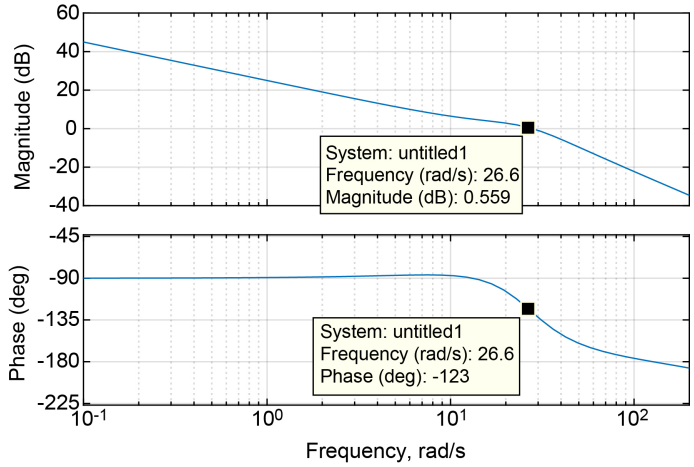

Figure 24.—Bode plot of the OL TF for the PID control design.

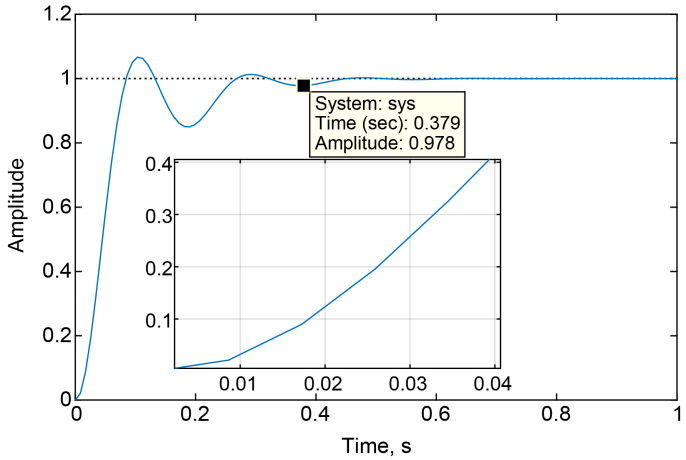

Figure 25.—Step response of the feedback system with PID control.

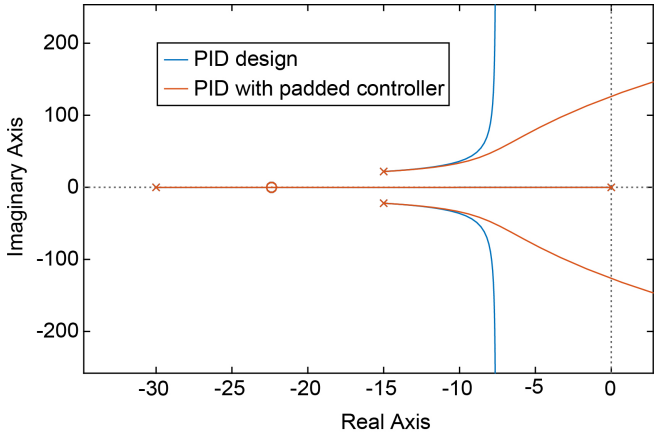

Figure 26.—Root locus of PID control design with unpadded control, and the low frequency RL with padded control.

The step response of the PID control system design is shown in Figure 25. The design about meets the settling time spec (actually it takes slightly longer; the design just met the spec as it was tuned in the MATLAB® graphical tool, before the addition of the padding pole). The initial response time, after some delay shows that the system speed is about 15 units/sec, which is also significantly less than that achieved by RL or LS designs. Figure 26 shows the RL of this PID design in blue. This shows that there is no way to achieve as fast a response as that obtained with RL or LS control designs as the RL of the PID design does not bend towards the LHP. In order to achieve the same or similar response to these other two designs, one less zero would be needed in the OL TF than the number of poles (remember the plant has three poles and the PID has one pole at the origin and two zeros), which would exclude PI or PID control for this example problem. Also as shown in Figure 26, the original PID controller has its poles going to infinity in the left hand plane, which means that for increasing gain this system will not become unstable, but it will become oscillatory. For the padded design this system will become unstable as the gain increases, as the poles of this design cross into the RHP. Generally, the padded design cannot be avoided, as even MATLAB® will insert a pole(s) as needed to keep the controller TF proper. As mentioned before, an unpadded controller design can possibly be obtained by tightly integrating the controller with the plant, as will be shown in Appendix A.

In general, there are no reasonable comparisons that can be made between PID and RL or LS controls design methodologies, as the RL and LS techniques have no restriction on the number of poles and zeros that can be used in a design, while PI and PID are restricted to a pole at the origin and one or two zeros, respectively. As seen in the example covered, PID control cannot achieve the bandwidth and the noise rejection specs, compared to the RL or LS designs, because it doesn't have sufficient zeros.

5.0 Conclusion

In this paper, approaches were introduced to simplify the design of control systems using the Root Locus and the Loop Shaping control design techniques. The Root Locus control system design covered in literature is often not easy to understand. However, the approach covered in the paper is relative easy to apply. The same is true for the Loop Shaping control approach covered in the paper. These two control design techniques can be compared to each other, but in essence how good of a controls design can be achieved with either approach is only limited by the skills of the controls designer. A comparison of these two methods is carried out against Proportional Integral Derivative (PID) control, which demonstrates that the performance of PID control is limited. That is because in general PID control is a subset of these other two methods. The appendices in the paper show: i) how a control system design can be achieved that is inherently robust or ultra-stable provided the plant can be integrated with the controller as a single Transfer Function; ii) how to design a model following control system that improves control system robustness and can also take full advantage of the speed of its actuation system in cases where the response time of the control system is required to be slower; and iii) how to use the knowledge gained to design feedback controls for more realistic and perhaps more complicated plants systems, which also serves to further reinforce the design approaches covered in the paper.

Appendix A

In the RL section it was shown how control designs can be produced that are inherently stable for any value of the proportional gain, provided that the combined controller and plant TF has only one more pole than the number of zeros. Except for isolated cases where the plant TF has only one more pole than the number of zeros, this is not possible to achieve with typical digital control where it becomes necessary for all TFs to be proper. The purpose of the appendix is to show how a control design can potentially be achieved that meets this criterion (a combined TF of one more pole than the number of zeros), by tightly integrating the controller and the plant TF.

The appendix covers an example that describes the process of developing a tightly integrated control system design. Theoretically, such designs can facilitate the RL shape described in the paper, whereby the RL bends and extends into the left plane to allow an ultra-stable or robust design, independent of the value of the OL proportional gain and for large variations of pole/zero locations. While theoretically possible for such a stable and robust control system design to be achievable, extra care must also be taken to include higher frequency process dynamics, and also not to create extra dynamics in the process of implementing the controller design, which is not necessarily an easy task. Since it is difficult to account for high frequency dynamics, if such dynamics exist in a tightly integrated control system and are not accounted for, the system can still be robust to large changes in the system proportional gain.

Say we have a control system with an OL TF, $\boldsymbol{G_o(s)} = \frac{(s+a)(s+b)}{s(s+c)(s+d)} = \frac{Y(s)}{E(s)}$ (omitting the proportional gain for simplification of the state space diagram), where $Y(s)$ is the output and $E(s)$ is the input or the error. Say that the two zeros with the pole at the origin are part of the controller design, whereas the other two poles are part of the plant TF. The controller TF in such a system is not proper, but this will not be a problem if the plant and the controller design can be successfully integrated into a single system. Notice that this OL TF with one more pole than the number of zeros will have a loop shape that bends and extends into the LHP, according to the discussion and the control design covered in the RL section. The question here is how such an OL TF can be implemented without separating the controller and the plant TFs, which will necessitate a proper controller TF design and therefore, a loop that will not have the desirable shape. The solution here is to implement the OL TF in the form of a state space diagram, which permits a tight coupling of the controller with the plant.

The above TF can be expressed as $\boldsymbol{Y(s)[s^3+(c+d)s^2+cds]=E(s)[s^2+(a+b)s+ab]}$ and converting to the equivalent differential equation, $\boldsymbol{\dddot{y} + (c+d)\ddot{y} + cd\dot{y} = \ddot{e} + (a+b)\dot{e} + abe}$. In order to facilitate a space state diagram form, the state variables need to be rearranged such that the highest derivative of the output, together with all the derivatives of the input, appear on the LHS of the equation as

$$\boldsymbol{\dddot{y} - \ddot{e} - (a+b)\dot{e}} = abe - \boldsymbol{(c+d)\ddot{y} - cd\dot{y}} \tag{A.1}$$

With the consideration that the expression on the left hand side of the equation constitutes the overall derivative of the equation, an integrator is placed in front of such an input and sequentially integration is carried out, while at the same time summing blocks are used to eliminate non-derivative terms until finally, the output variable *y* is obtained as shown in the diagram in Figure A.1. After this process is completed, a summing block is added at the input to feed back the terms that will satisfy the RHS of Equation (A.1), which generates the derivative or the expression on the LHS of this equation. Except for the extra term $\boldsymbol{(c+d)\dot{e}}$, that cannot be eliminated in this state space diagram, which prevents closure, as shown in Figure A.1.

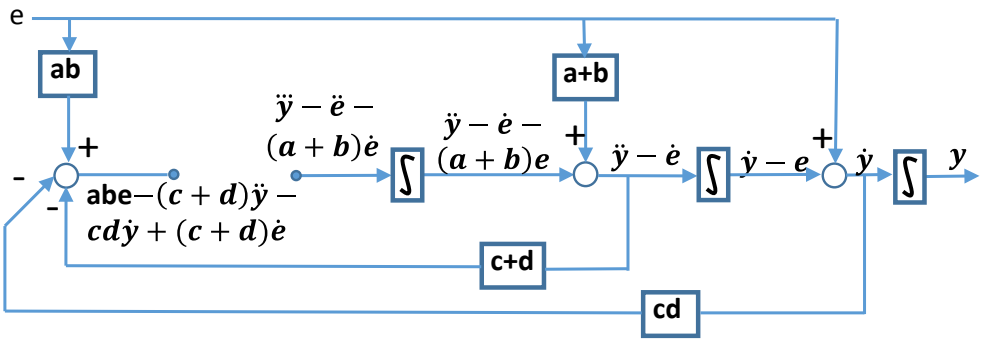

Figure A.1.—State space diagram of Equation (A.1) - incomplete.

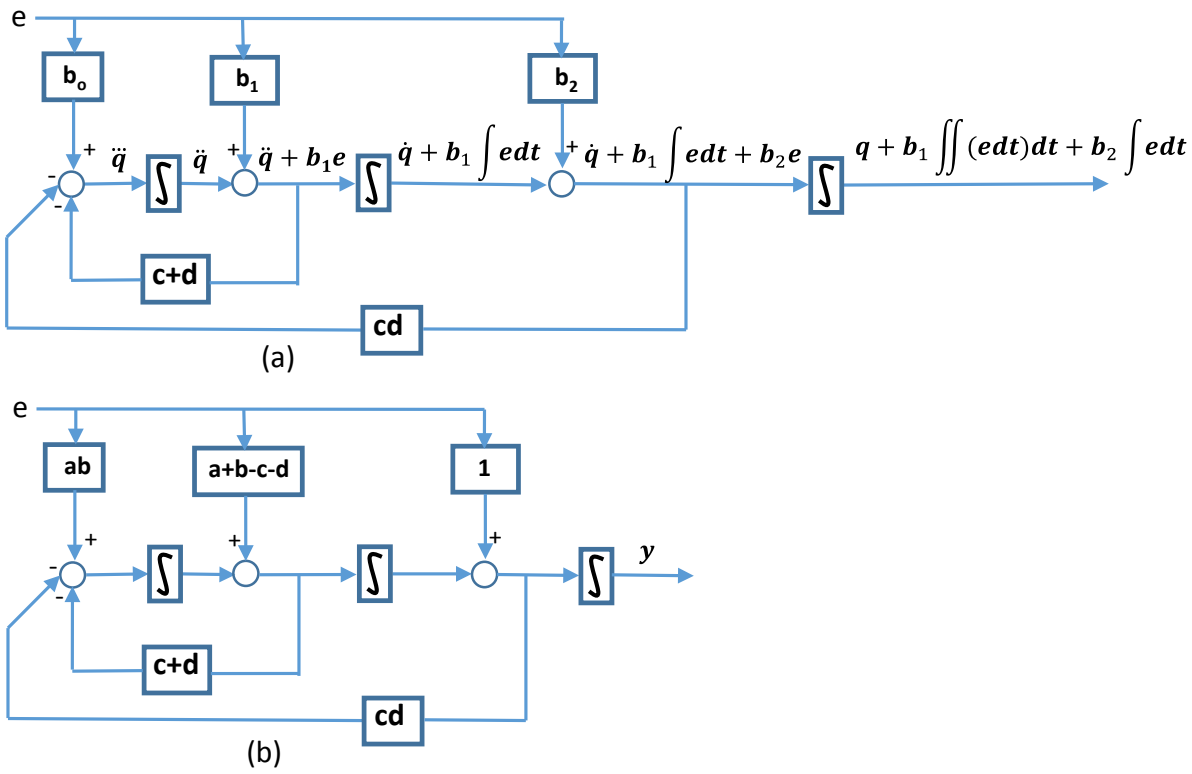

Figure A.2.—a) Assumed state space form of Equation (A.1), (b) actual state space diagram of Equation (A.1).

Instead, a generic state space form will be assumed for feeding the input *e* into the state variables as shown in Figure A.2(a), with constants to be evaluated. With the input to the first integrator $\ddot{q}$, the values of other points in Figure A.2(a) are indicated. This block diagram is a representation of the differential equation

$$\ddot{q} = -(c+d)\ddot{q} - cd\dot{q} + [b_o - (c+d)b_1 - cdb_2]e - cdb_1 \int edt \tag{A.2}$$

With the understanding that the output of the simulation in Figure A.2(a) should be equal to *y* gives

$$q = y - b_1 \iint (edt)dt - b_2 \int edt \tag{A.3}$$

Then

$$\dot{\boldsymbol{q}} = \dot{\boldsymbol{y}} - \boldsymbol{b_1}\int \boldsymbol{e}\boldsymbol{dt} - \boldsymbol{b_2}\boldsymbol{e} \tag{A.4}$$

$$\ddot{\boldsymbol{q}} = \ddot{\boldsymbol{y}} - \boldsymbol{b_1}\boldsymbol{e} - \boldsymbol{b_2}\dot{\boldsymbol{e}} \tag{A.5}$$

$$\dddot{\boldsymbol{q}} = \dddot{\boldsymbol{y}} - \boldsymbol{b_1}\dot{\boldsymbol{e}} - \boldsymbol{b_2}\ddot{\boldsymbol{e}} \tag{A.6}$$

Substituting Equations (A.2), (A.4) and (A.5) into Equation (A.6) yields

$$\begin{aligned} -(\boldsymbol{c}+\boldsymbol{d})[\ddot{\boldsymbol{y}} - \boldsymbol{b_1}\boldsymbol{e} - \boldsymbol{b_2}\dot{\boldsymbol{e}}] - (\boldsymbol{c}+\boldsymbol{d})\boldsymbol{b_1}\boldsymbol{e} - \boldsymbol{cd}\left[\dot{\boldsymbol{y}} - \boldsymbol{b_1}\int \boldsymbol{e}\boldsymbol{dt} - \boldsymbol{b_2}\boldsymbol{e}\right] - \\ -\boldsymbol{cdb_1}\int \boldsymbol{e}\boldsymbol{dt} - \boldsymbol{cdb_2}\boldsymbol{e} + \boldsymbol{b_o}\boldsymbol{e} = \dddot{\boldsymbol{y}} - \boldsymbol{b_1}\dot{\boldsymbol{e}} - \boldsymbol{b_2}\ddot{\boldsymbol{e}} \end{aligned} \tag{A.7}$$

Collecting terms,

$$\dddot{\boldsymbol{y}} - \boldsymbol{b_2}\ddot{\boldsymbol{e}} - [\boldsymbol{b_1} - (\boldsymbol{c}+\boldsymbol{d})\boldsymbol{b_2}]\dot{\boldsymbol{e}} = \boldsymbol{b_o}\boldsymbol{e} - (\boldsymbol{c}+\boldsymbol{d})\ddot{\boldsymbol{y}} - \boldsymbol{cd}\dot{\boldsymbol{y}} \tag{A.8}$$

Comparing Equation (A.8) with Equation (A.1), terms b_o, b_1, and b_2 are calculated by equating like terms, and they are

$$\boldsymbol{b_o} = \boldsymbol{ab},\ \boldsymbol{b_1} = \boldsymbol{a}+\boldsymbol{b}-\boldsymbol{c}-\boldsymbol{d},\ \boldsymbol{b_2} = \boldsymbol{1}.$$

The complete diagram is shown in Figure A.2(b).

Following the same procedure to draw the state space diagram of the plant TF in this example (before the controller is inserted), the state space diagram shown in Figure A.3 is obtained. Comparing this diagram with that shown in Figure A.2(b), it can be seen that the controller in this example system can be implemented and integrated with the plant by adding one integrator at the output of the plant, and by inserting the summing blocks with the gains shown in Figure A.2(b) for the error input. The summation of these blocks shown would be inserted directly into the plant, assuming that all the states of the plant are observable and accessible.

Such tightly integrated controller/plant TFs can be developed with any system that can be designed to have only one more pole than the number of zeros. Then, by utilizing the RL design covered in the paper, such control systems can potentially result in ultra-robust control designs or at least result in control designs that are stable to large variations in the system proportional gains. The drawback for such tightly integrated control designs is that it might be necessary that at least part or the control law implementation be done in the native environment of the plant design. If the plant happens to be an electrical system, the controller can be tightly integrated with the plant using an analog circuit for the controller, while for a system like a spring-mass system, the controller may need to be also represented by a mass-springs system.

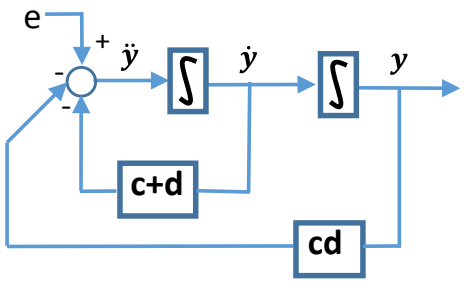

Figure A.3.—State space diagram of the example plant TF.

Appendix B

In this appendix an example control system design will be covered for a system whose response time (due to requirements) is relatively slow compared to the speed of its actuator, with the design objective to meet the response time requirement while at the same time take maximum advantage of the speed of the actuation system.

Say that in this example the settling time of the control system is required to be 5 s, given a plant TF $\mathbf{G_p(s)= (9542s+ 20770)/(s^2+4.852s+5.171)}$. For a 5 s first order type system response (i.e., $\omega_n/(s+\omega_n)$), $\omega_n \approx \mathbf{4/5} = \mathbf{0.8}$ rad/s, where 4 is the number of time constants it takes for the response to settle or to achieve 98% of its steady state value. Also, say that the actuator TF, Ga(s), of the process has a 6 Hz bandwidth or roughly 37 rad/s. Based on the actuator speed alone and the LS design approach covered in Section 3.0, the desired OL TF can be chosen as $\mathbf{G_d(s)=15(s/1.5+1)/[s(s/3.7+1)]}$, which will provide for a bandwidth of 37 rad/s, a mid-frequency gain of approximately 20 dB, and more than adequate stability margins. For this desired OL TF, a controller design based on the approach discussed in Section 3.0 will be, $\mathbf{G_c(s)=(9.102\times10^6s^5+7.987\times10^8s^4+1.728\times10^{10}s^3+8.844\times10^{10}s^2+1.609\times10^{11}s+9.665\times10^{10})/(1.959\times10^7s^5+1.599\times10^{10}s^4+3.307\times10^{12}s^3+1.901\times10^{13}s^2+2.588\times10^{13}s)}$. Notice that without including the actuator TF and because in this example the plant TF has one more pole than zero, it is possible to design a controller with a proper TF (equal number of poles and zeros) that results in a robust control system design for any uncertainty in the proportional gain, according to the RL design approach covered in the paper. Typically however, in an actual control system design, the actuator dynamics would need to be included.

In order to design the control system to take full advantage of the actuator speed while at the same time satisfying a slower response time as in this example, a model following control system design structure is chosen as shown in Figure B.1. The model response that the control system is designed to follow is that of the reference model shown in Figure B.1, which provides for the desired response time and a first order type response in this case. The purpose of the external feedback gain is to tune the control system response to follow that of the reference model; the higher this gain is, the closer these two responses will match (up to a point, before oscillations begin to take place). The filter at the input is used to slow down the initial step command in order to allow this close matching of the two responses to occur without any oscillations. As with most control systems, a sharp step command input is not required.

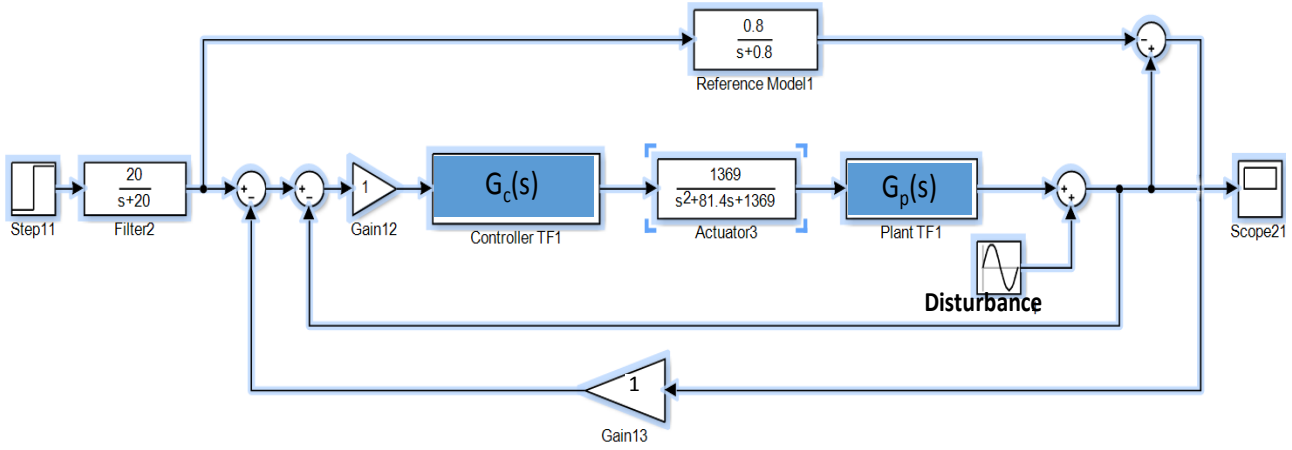

Figure B.1.—Model following control structure for LS design with an actuation system faster than the required response time.

Bode plots of the OL TF ($G_c(s)*G_a(s)*G_p(s)$) for the control system shown in Figure B.1 can be plotted as before to evaluate its performance. This will not be done here, since the process of doing so is the same as that covered in the body of the paper. Figure B.2 shows a step response of the reference model against that of the LS-Model Following Control (LS-MFC) design, which shows that the feedback control system response closely follows that of the reference model. Figure B.3 shows the disturbance rejection capability of the LS-MFC for a disturbance of 1 unit amplitude at a frequency of 3 rad/s. The figure shows the actual disturbance, the output of the LS control design without the model following, and the output of the LS-MFC shown in Figure B.1. The LS control design attenuates the disturbance by approximately 20 dB as expected at the mid-frequency range based on the design approach covered in the paper. The LS-MFC design in this example however, attenuates the disturbance by approximately 43 dB (see the inset in Figure B.3), which is substantially more.

If the control system was designed to meet the 5 s settling time requirement without taking advantage of the speed of the actuator, there would have been significantly less disturbance rejection at the frequency of 3 rad/s, as the bandwidth of the control system would have been only about 6 rad/s. Anytime the bandwidth of the control system is increased however, as in this design example, care must be taken to make sure that the plant model includes the appropriate dynamics.

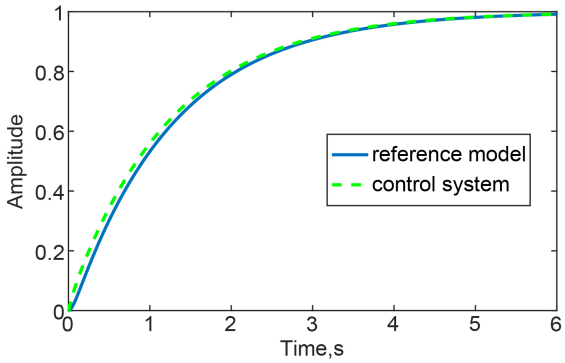

Figure B.2.—Response time of model following control system.

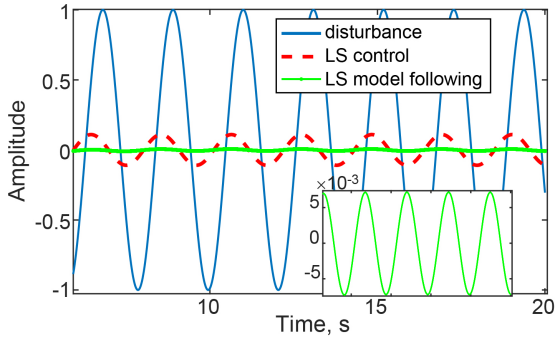

Figure B.3.—Disturbance rejection of LS control and of LS model following control system design.

For this system, the gain at the input of the controller represents gain uncertainty, and for high gains the control system shown in Figure B.1 will go unstable. The reason for this is because the robustness of the design is compromised due to the additional poles (actuator poles), as covered in the RL section. To improve the robustness of the design, a low pass filter can also be added to the external feedback, like $\mathbf{G_F(s)=5/(s+5)}$, which will provide gain tolerance or robustness for up to an order of magnitude for gain variations, and also provide significant tolerance to uncertainty in the process dynamics. In fact, the same filter can also replace the input filter shown in Figure B.1.

To demonstrate the improvement in the robustness of the control system using the model following control structure, Figure B.4(a) shows the response of the control system for the original gain, K (Gain12 in Figure B.1), and 10 times this gain. Also, the filters discussed above were added for this simulation, with an external feedback gain value of 1 (this value suffices with the addition of the filters), and with the reference model replaced with the feedback TF of the desired control system (i.e., $\mathbf{G_d(s)=15(s/1.5+1)/[s(s/3.7+1)]}$; $\mathbf{G_{Ref}=feedback(G_d,1)}$). To emphasize that these improvements using the model following control structure with the LS design are not unique to this particular plant, Figure B.4(b) shows such responses for the example plant covered for LS in Section 3.2 with the controller $G_{c2}(s)$ and its corresponding $G_d(s)$ feedback system for the reference model (i.e., $G_{c2}(s) = \mathrm{K}\frac{(s+5)(s+30)(s^2+30s+709)}{s(s+10)(s/1100+1)(s/1300+1)}$ and $\mathbf{G_d(s) = 50(s/5+1)/[s(s/10+1)]}$). The bandwidth of the filters should be sufficient such that the settling time requirement is not compromised. The uncertainty proportional gain values of 10 and 20 shown in Figure B.4(a) and (b) are about at the limit that these control designs can tolerate, respectively, without going unstable.

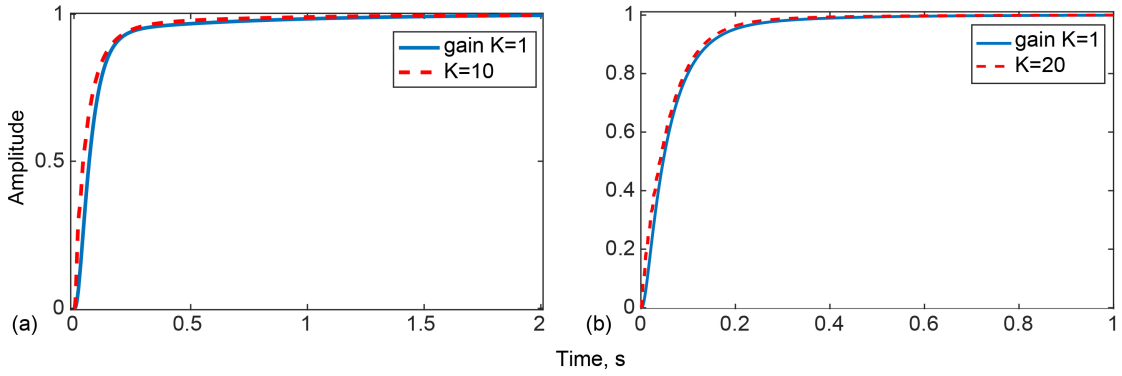

Figure B.4.—Response time of model following control system with gain uncertainty (a) for the example in this appendix, (b) for the example covered in the LS section of the paper.

Appendix C

In this appendix another example is demonstrated for feedback control system design using the RL, LS, and PID control methods. The objective is to make this example more realistic, perhaps a little more complicated in terms of a control process, while emphasizing and reinforcing some of these control design concepts.

For the mechanical system shown in Figure C.1, the objective is to control its displacement, $x_1(t)$, using the force, $f(t)$. After drawing its two free body diagrams by assuming static equilibrium, summing up the forces, taking the Laplace transforms of the differential equations, and using Matrix algebra to solve the system (not shown since the objective here is control design), the TF of this displacement with respect to the applied force is

$$\frac{X_1(s)}{F(s)} = \frac{0.25(s/1.67+1)}{(s/4.81+1)(s/2.18+1)(s^2/0.95+1.51s/0.95+1)}$$

Say the force is applied via an actuator that has the following TF, with an actuator speed limit of 10 units/s or according to the LS design method, designed to a crossover frequency limit of 10 rad/s.

$$G_A(s) = \frac{1}{(s/5+1)}$$

For additional specs, say, the control designs should take maximum advantage of the speed of the actuator (fast response), with good disturbance rejection of approximately 20 dB gain at mid-frequency, with an overshoot of less than 20%, and with PM and GM of greater than 50° and 10 dB, respectively.

C.1 Root Locus Control Design

Using the RL control design methodology covered in this paper, it is recognized that the combined plant TF has one zero and five poles, plus one more pole that is needed at the origin for zero SS error to a step input command. Based on the RL design approach, four zeros will be needed in the controller design (i.e., an OL TF design with one less zero than the number of poles). This is in order to bend the RL trajectory to the left to allow the control system to meet the desired cross-over frequency and therefore,

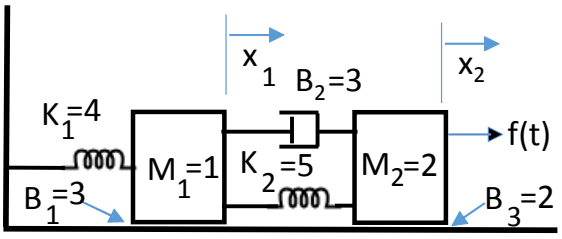

Figure C.1.—Mechanical system to control displacement x_1 using force f(t); *K*-spring constant in N/m; *B*-damper in N-s/m; *M*-mass in kg.

meet the desired speed limit or remain slightly below. As the placement of the leftmost zero primarily impacts the frequency where the complex poles of the plant will loop around and intersect the real axis (impacts the natural frequency, ω_n, of these poles), and as the target for this intersection is somewhere near 10 rad/s, the leftmost zero is placed at 5.7 rad/s in this design (a little trial and error). The rest of the zeros are placed relatively close together, except perhaps for the lowest frequency zero, which impacts the settling time. So for this design, the controller zeros are placed at *Z*1=5.7 rad/s, *Z*2=5 rad/s, *Z*3=3 rad/s, *Z*4=1 rad/s. The RL for this OL TF design with a process proportional gain of 1 is shown in Figure C.2. For the selected point shown on the RL plot for the CL conjugate pole locations, it can be seen that the proportional gain is 42, while the damping is good.

The bode plot of the OL TF of this RL design with the proportional gain of 42 is shown in Figure C.3, which as seen exceeds the limit requirement for the cross-over frequency of 10 rad/s. The proportional gain of this design is therefore reduced by the magnitude of 3.96 dB that this gain exceeds the requirement, as $\log^{-1}[20\log(3.96)] = 10^{3.96/20} = 1.58$. As shown, the adjusted OL TF design (dashed line) meets the cross-over limit and has a PM of approximately 76° and infinite GM. The mid-frequency gain for disturbance rejection in this adjusted design is approximately 27 dB, which meets or exceeds the spec.

Based on that, the resulting controller TF, including the required padding poles to make the TF proper, is as follows.

$$G_c(s) = \frac{106.51(s/5.7+1)(s/5+1)(s/3+1)(s/1+1)}{s(s/100+1)(s/110+1)(s/120+1)}$$

This design with the padded controller is also shown in Figure C.3. Notice the controller gain is K_c=42/(Kp*1.58), and for the bode plot $G_p(s) = \frac{X_1(s)}{F(s)} G_A(s)$, with the original gain K_p=0.25. This final control design still meets the specs with a PM of approximately 60°, a GM of approximately 19 dB and a

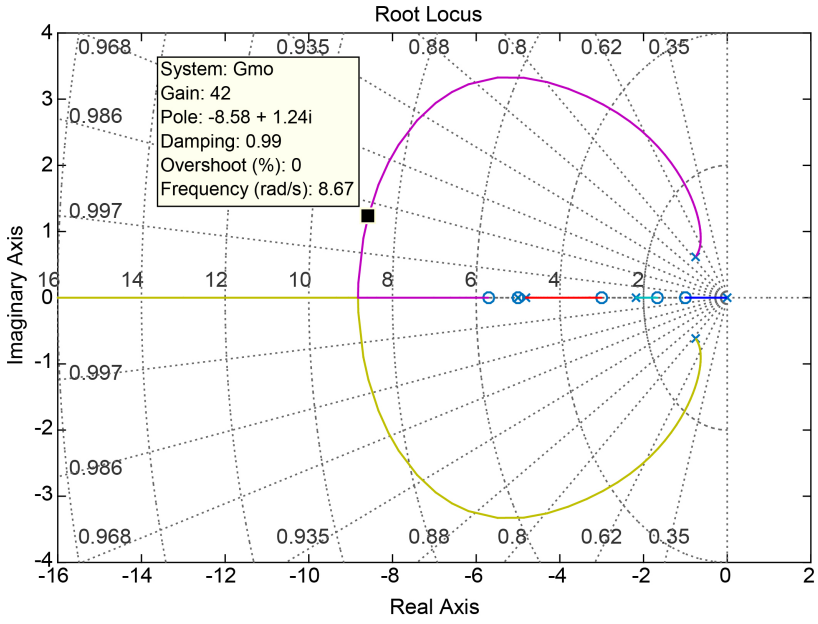

Figure C.2.—Root locus of the plant TF with a proportional gain of 1.

mid-frequency gain (up to a frequency of 1 rad/s) of better than 20 dB. The padding poles could be moved to higher frequencies if the desire is to keep the PM of the original design. The step response ($x_1(t)$ – displacement in meters) of the feedback system is shown in Figure C.4, which shows that the overshoot spec of less than 20% is also met in this design. The settling time is approximately 0.8 s, which is relative fast; the result of taking nearly maximum advantage of the actuator speed in this design, and the placement of the lowest frequency zero. Zooming in on the initial or the fastest portion of the response as shown in the inset, the response is approximately 8 units or 8 m/s, which is close to but does not exceed the actuator limit, and perhaps still offers some room to increase the bandwidth of the control design.

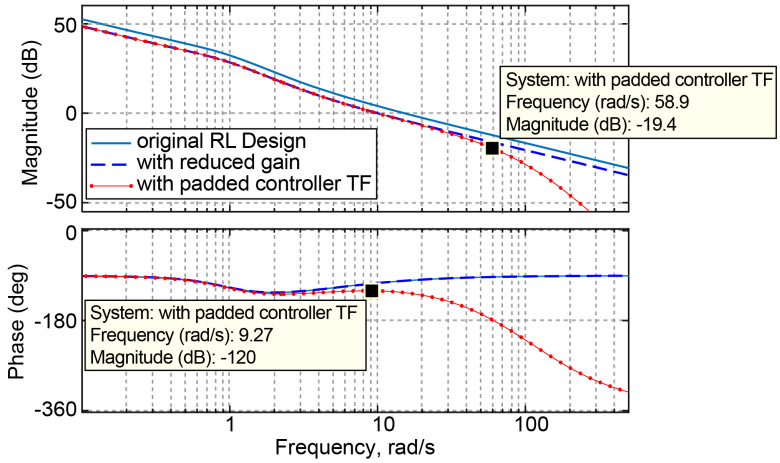

Figure C.3.—Bode plots of the OL TF design and that for the reduced gain.

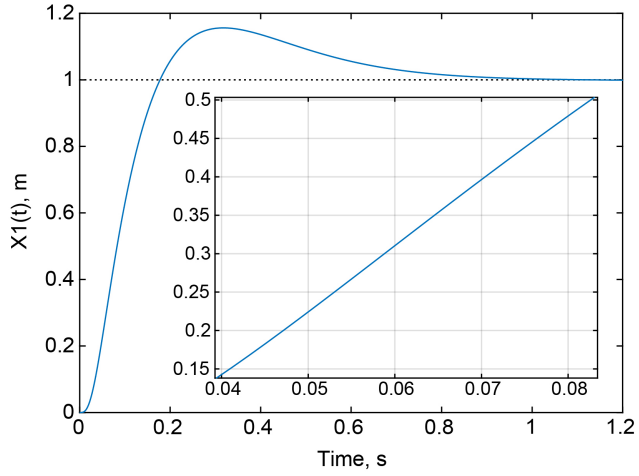

Figure C.4.—Control system step response for the RL design, and the inset showing the initial speed of the system.

C.2 PID Control Design

For the PID control design, the process is the same as described in Section 5.0, and for this process the PID controller design that seems to perform the best in terms of meeting the specs, including a padding pole to make the TF proper, is as follows.

$$G_c(s) = \frac{K_I\left(\frac{K_D}{K_I}s^2 + \frac{K_P}{K_I}s + 1\right)}{s\left(\frac{s}{100} + 1\right)}$$

with K_p=10.86, K_i=5.25, K_d=5.61.

Shown in Figure C.5 is the bode plot of this design, which meets the requirements, but with a smaller control bandwidth or crossover frequency. For instance, in this design the approximately 20 dB mid frequency gain is met, however, at a frequency of about 1/10th that of the RL control design, which means that this design will have significantly less disturbance rejection capability. The settling time in this design is considerably slower and the speed of the system is nowhere near that obtained in the RL control design (Figure C.6). That is, the PID control design is not able to take maximum advantage of the speed of the actuator in this system.

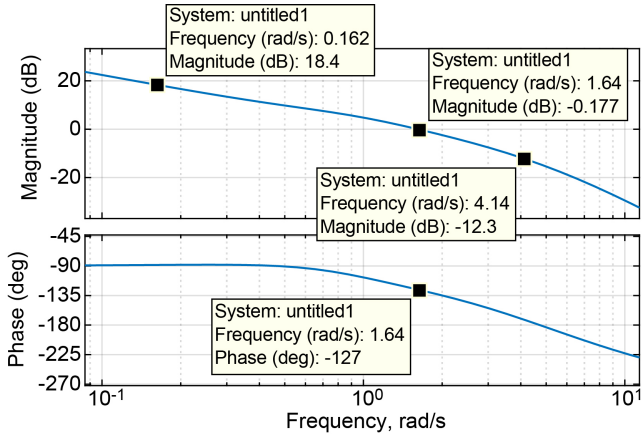

Figure C.5.—Bode plots of the PID control design.

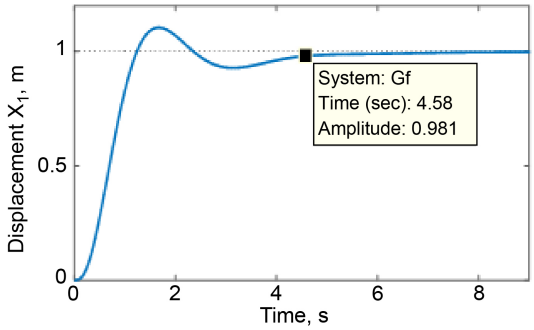

Figure C.6.—Control system step response for the PID control design.

C.3 Loop Shaping Control Design

For the LS control design in this example, a different control design approach will be demonstrated from that described in Section 3.0, which normally results in a lower order controller for cases in which the plant dynamics are not significantly underdamped. In this LS control design approach the design for the desired OL TF, G_d, will be the same as that shown in Section 3.1. However, for the actual OL TF design to match the bode plot of G_d, the approach here is to design the controller for the corresponding OL gain to match the gain of G_d, starting from low frequency – step-by-step, and without cancelling the plant dynamics. First, the low frequency factors in $G_d(s)$, Kc/s, (i.e., $Kc=K_d/K_p$) are kept in the first attempt of the controller design to match these OL gains. After that, the 3 dB separation in these two gains is to be found successively (one at a time), and a zero is inserted at these frequencies (one at a time) and the process is repeated in order to match these gains at progressively higher and higher frequencies, up to the cross over frequency. If the bode gain of this design happens to be higher than that of the desired OL gain, G_d, poles will be inserted instead of zeros.

The design of G_d in this example is carried out here with its zero selected at the frequency of 7.5 rad/s, which is higher than the recommended frequency range of its zero of 1/4th to ½ the frequency of its pole. Here again, the frequency of the pole in the TF $G_d(s)$ is placed at 1/10th the cross over frequency. The placement of the zero at higher than the recommended frequency is done here independently, for the purpose of speeding the response; this will somewhat compromise the robustness of the system. The recommended frequency range of this zero causes the control system response to transition to a first order type response somewhere at near 90% of the response, for enhanced system stability and robustness. Based on that, the desired OL gain G_d is as follows.

$$G_d(s) = \frac{7.5(s/0.75+1)}{s(s/1+1)}$$

The matching process of the OL TF of the control system design with the bode gain of $G_d(s)$ in steps is shown in Figure C.7. The topmost frequency response is that of $G_d(s)$, while the rest of the responses show progressively increased matching with $G_d(s)$, starting from the bottommost response (red) and moving up. The final attempt matches the response of $G_d(s)$ up to the cross-over frequency of 10 rad/s, almost indistinguishably for this resolution, with a slight difference shown in phase matching (blue vs. cyan colors). The controller design for these successive matching steps are as follows: $G_c(s)$= 30/s; 30(s/0.75+1)/s; 30(s/0.75+1)(s/1.355+1)/s; 30(s/0.75+1)(s/1.355+1)(s/2.9+1)/s; 30(s/0.75+1)(s/1.355+1)(s/2.9+1)/s)(s/8.5+1)/s. Notice the controller successive designs displayed here do not constitute proper TFs. However, each of these expressions together with the plant is handled as a single TF to generate the responses in Figure C.8 (ex., **bode(30*(s/0.75+1)/s)*Ga*Gp)**). Thus, for this design the controller TF, including the padding poles at 10x or more the cross-over frequency is

$$G_c1(s) = \frac{30(s/0.75+1)(s/1.355+1)(s/2.9+1)(s/8.5+1)}{s(s/100+1)(s/120+1)(s/140+1)}$$

The feedback system step response with this controller design is shown in Figure C.8, with the inset showing a settling time of approximately 0.23 s. For the desired OL TF, $G_d(s)$, the settling time instead, was 0.6 s. The difference is due to the underdamped dynamics in the process and the matching performed for the control system design, which does not exactly match at the frequency of the process underdamped dynamics. The initial response or the fastest speed of the process (not shown here) is approximately 8.3 m/s for this design, which is near, but under the limit of 10 m/s that is specified.

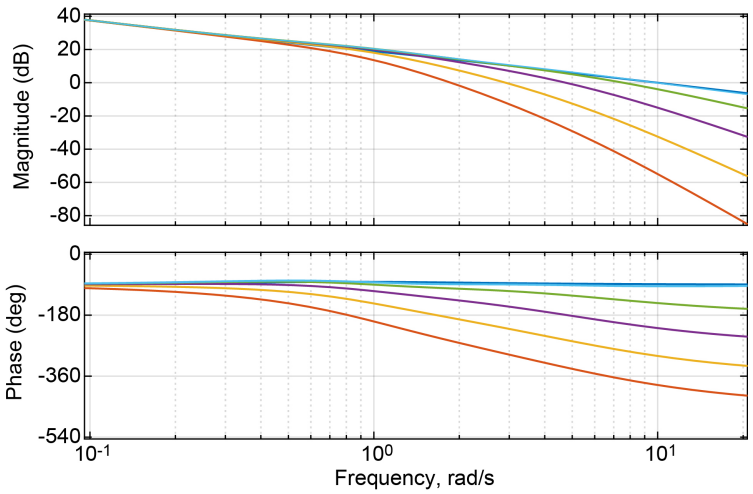

Figure C.7.—Frequency response of $G_d(s)$, and that of the designed control system OL TF, in successive attempts to match these responses.

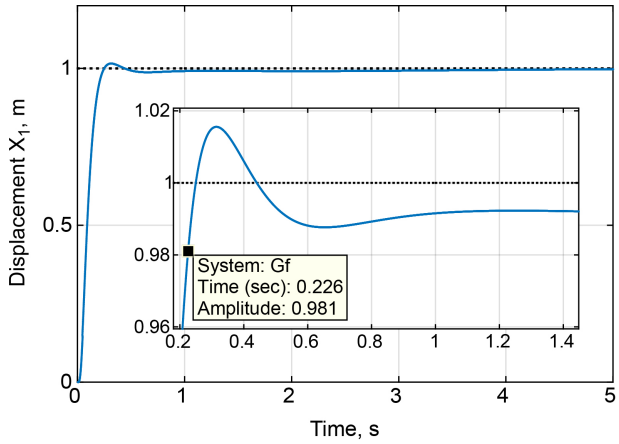

Figure C.8.—Control system step response for the LS control design.

References

1. Franklin, G. F.; Powell, D. J.; Emami-Naeini, A.; "Feedback Control of Dynamic Systems," Book – Pearson Education, 7th Edition, 2015.
2. Kopasakis, G.; "Feedback Control Systems Loop Shaping Design with Practical Considerations," NASA/TM—2007-215007.
3. Kopasakis, G; Connolly, J. W.; "Shock Positioning Controls Design for a Supersonic Inlet," 45th AIAA/ASME/SAE/ASEE Joint Propulsion Conference & Exhibit, Denver, Co, 2-5 Aug. 2009.
4. Richter, H., Lecture 15: Relative Stability: Gain and Phase Margins Frequency Domain Performance Loop Shaping Design, http://academic.csuohio.edu/richter_h/courses/mce441/mce441_15_hand.pdf.